Peroxisomes attenuate cytotoxicity of very long-chain fatty acids

Hanif Ali[a, b], Miyu Kobayashi[a], Katsuya Morito[b], Rumana Yesmin Hasi[a], Mutsumi Aihara[a], Junji Hayashi[a], Ryushi Kawakami[a], Koichiro Tsuchiya[b], Kazunori Sango[c], Tamotsu Tanaka[a,*]

[a]*Graduate School of Technology, Industrial and Social Sciences, Tokushima University, Tokushima, 770-8502, Japan*

[b]*Graduate School of Biomedical Sciences, Tokushima University, Tokushima, 770-8505, Japan*

[c]*Diabetic Neuropathy Project, Department of Diseases and Infection, Tokyo Metropolitan Institute of Medical Science, Tokyo, 156-8506, Japan*

*To whom correspondence should be addressed

e-mail: tanaka.tamotsu@tokushima-u.ac.jp

Abstract

One of the major functions of peroxisomes in mammals is oxidation of very long-chain fatty acids (VLCFAs). Genetic defects in peroxisomal β-oxidation result in the accumulation of VLCFAs and lead to a variety of health problems, such as demyelination of nervous tissues. However, the mechanisms by which VLCFAs cause tissue degeneration have not been fully elucidated. Recently, we found that the addition of small amounts of isopropanol can enhance the solubility of saturated VLCFAs in an aqueous medium. In this study, we characterized the biological effect of extracellular VLCFAs in peroxisome-deficient Chinese hamster ovary (CHO) cells, neural crest-derived pheochromocytoma cells (PC12), and immortalized adult Fischer rat Schwann cells (IFRS1) using this solubilizing technique. C20:0 FA was the most toxic of the C16–C26 FAs tested in all cells. The basis of the toxicity of C20:0 FA was apoptosis and was observed at 5 μM and 30 μM in peroxisome-deficient and wild-type CHO cells, respectively. The sensitivity of wild-type CHO cells to cytotoxic C20:0 FA was enhanced in the presence of a peroxisomal β-oxidation inhibitor. Further, a positive correlation was evident between cell toxicity and the extent of intracellular accumulation of toxic FA. These results suggest that peroxisomes are pivotal in the detoxification of apoptotic VLCFAs by preventing their accumulation.

Keywords:

Peroxisome disease

Very long-chain fatty acids

Peroxisome-deficient cells

Apoptosis

Abbreviations: ABCD1, ATP binding cassette subfamily D member 1; ALD, X-linked adrenoleukodystrophy; ALDP, adrenoleukodystrophy protein; BSA, FA-free bovine serum albumin; CHO, Chinese hamster ovary; DAPC, 1,2-diarachidoyl-sn-glycero-3-phosphocholine; DAPI, 4',6'-Diamidino-2-phenylindole; DMEM, Dulbecco's modified Eagle's medium; FAs, fatty acids; FAMEs, fatty acid methyl esters; FBS, fetal bovine serum; GC, gas chromatography; IFRS1, immortalized adult Fischer rat Schwann cell; IP, isopropanol; LCFAs, long-chain fatty acids; MU-VLCFAs, monounsaturated very long-chain fatty acids; Na, NaOH; PC12, neural crest-derived pheochromocytoma cells; ROS, reactive oxygen species; S-VLCFAs, saturated very long-chain fatty acids; TDYA, 10,12-tricosadiynoic acid; TLC, thin layer chromatography; VLCFAs, very long-chain

fatty acids; ZS, Zellweger syndrome.

1. Introduction

Peroxisomes are multifunctional organelles found in virtually all eukaryotic cells. These organelles are essential in the degradation and synthesis of lipid molecules [1–4]. The central function of peroxisomes in mammals is the oxidation of fatty acids (FAs) that are not oxidized in the mitochondria. These include very long-chain fatty acids (VLCFAs, C≥20), long-chain dicarboxylic acids, branched-chain fatty acids, and certain xenobiotics [1–4]. Intact peroxisomal function is crucial for normal human development and the integrity of organic functions, including neurons, adrenal glands, liver, and kidneys. This functional requirement is evident from the fact that genetic defects in peroxisomal function lead to a variety of health problems called peroxisomal disorders [5–8].

Peroxisome disorders are classified into two groups: peroxisome biogenesis disorder and single peroxisomal enzyme deficiency. Zellweger syndrome (ZS) is a typical peroxisome biogenesis disorder and the most severe form of peroxisome disease. The characteristic clinical features of ZS are neuronal migration defects, dysmyelination and neural heterotopia [9–12]; currently, no treatment is available for recovery. Due to defects in peroxisome-assembly proteins, functional peroxisomes are absent in the cells of patients with ZS. As a result, abnormally accumulated VLCFAs are characteristically observed in these cells [9–12]. Acyl-CoA oxidase 1 and D-bifunctional proteins are enzymes involved in peroxisomal β-oxidation of FA. Peroxisome disease caused by a functional deficiency of these enzymes is classified as a single peroxisomal enzyme deficiency. The resulting inability of peroxisomal β-oxidation leads to VLCFAs accumulation and causes severe neurodegeneration [9–11,13].

X-linked adrenoleukodystrophy (ALD) is the most common peroxisomal disease. ALD is caused by defects in the ATP binding cassette subfamily D member 1 (ABCD1) genes, which encodes adrenoleukodystrophy protein (ALDP), a peroxisomal membrane protein [14–20]. ALDP transports VLCFAs (as VLCFA-CoA) into the peroxisome [14–20]. The loss of function of ALDP leads to elevated levels of VLCFAs in the plasma and tissues [21–36]. The accumulation of saturated (S)-VLCFAs, specifically C24:0 and C26:0 FA, is a characteristic feature of this disease. Typical symptoms of ALD are adrenal insufficiency and neurodegenerations, such as demyelination with inflammation and oxidative damage [37–41].

Excess VLCFAs (C24:0 and C26:0 FA) induce toxicity in several neural cell types. These include plasma membrane changes, oxidative stress, and lysosomal and mitochondrial dysfunctions [42–51]. These observations support the view that the accumulation of VLCFAs is a causative event leading

to neurodegeneration. However, this assumption is too simplistic as ALD patients with elevated VLCFAs in the plasma can have mild or no neuronal symptoms. The relationship between accumulation of VLCFAs and the progression of peroxisome disease symptoms, such as demyelination/neurodegeneration, remains obscure.

To clarify the relationship between the accumulation of VLCFAs and the symptoms of peroxisome disease, it is important to understand the effect of VLCFAs on the functions of different cells, including myelinating cells. However, biological experiments using VLCFAs are hampered by their extremely low aqueous solubility. Recently, we developed a method for dispersing VLCFAs in aqueous medium. The method was based on the formation of a VLCFA/albumin complex in the presence of a small amount of alcohol in the albumin solution under warm (37 °C) conditions [52].

In this study, we demonstrated that our method is applicable to the solubilization of tested all long-chain fatty acids (LCFAs) and VLCFAs into culture medium. Experiments were performed to clarify the effect of these FAs on Chinese hamster ovary (CHO) cells with or without peroxisomes, neural crest-derived pheochromocytoma cells (PC12), and immortalized adult Fischer rat Schwann cells (IFRS1). We found that a certain kind of VLCFAs extensively accumulated in cellular lipids and displayed strong cytotoxicity. We also demonstrated that peroxisomes are pivotal in the detoxification of apoptotic VLCFAs by preventing their accumulation.

2. Materials & Methods

2.1. Materials

FA-free bovine serum albumin (BSA), 10,12-tricosadiynoic acid (TDYA), arachidic acid (C20:0 FA), paullinic acid (C20:1 FA), arachidonic acid (C20:4 FA), docosahexaenoic acid (C22:6 FA), tricosanoic acid (C23:0 FA), nervonic acid (C24:1 FA), pentacosanoic acid (C25:0 FA), and hexacosanoic acid (C26:0 FA) were obtained from Sigma-Aldrich (St. Louis, MO, USA). Palmitic acid (C16:0 FA) and stearic acid (C18:0 FA) were purchased from Tokyo Kasei Co. Ltd. (Tokyo, Japan). Oleic acid (C18:1 FA) was purchased from Nacalai Tesque (Kyoto, Japan) and 4',6'-Diamidino-2-phenylindole (DAPI) solution was purchased from Wako Pure Chemical Industries, Ltd. (Osaka, Japan). 1,2-Diheptadecanoyl-*sn*-glycero-3-phosphocholine (17:0/17:0 PC) and 1,2-Diarachidoyl-*sn*-glycero-3-phosphocholine (DAPC) were purchased from Avanti Polar Lipids (Alabaster, AL, USA). Behenic acid (C22:0 FA), erucic acid (C22:1 FA) and lignoceric acid (C24:0 FA) were purchased from Funakoshi Co. Ltd. (Tokyo, Japan). Proteinase K, RNase, 100bp DNA ladder, and BlueJuice™ Gel Loading Buffer were purchased from Invitrogen (Carlsbad, CA, USA). Thin layer chromatography (TLC) plates coated with silica gel (Art 5721; Merck, Darmstadt, Germany) were used. All other reagents used were of reagent grade.

2.2. Cell culture

Chinese hamster ovary (CHO-K1) cells were recruited from RIKEN Cell Bank (Tsukuba, Japan). CHO-zp102 cells were constructed by deleting *Pex5*, which encodes a peroxisome-targeting signal-1 receptor, as described previously [53,54]. The immortalized adult Fischer rat Schwann cell line (IFRS1) and the PC12 cell line were kindly gifted by Professor K. Watabe (Kyorin University). CHO cells were cultured and maintained in Ham's F-12 medium (Nacalai Tesque) containing 10% fetal bovine serum (FBS; Biowest, Noaillé, France), and 1% penicillin-streptomycin (Gibco BRL, Life Technologies, Inc., Rockville, MD, USA). IFRS1 cells were incubated with IMDM, GlutaMAX™ Supplement (Gibco BRL) containing 5% FBS, 20 ng/mL recombinant human heregulin-β (EMD Millipore, Billerica, MA, USA), 5 μM forskolin (Sigma-Aldrich), and an antibiotic antimycotic solution (100 U/mL penicillin, 100 μg/mL streptomycin, and 250 ng/mL amphotericin; Sigma-Aldrich). PC12 cells were incubated with Dulbecco's modified Eagle medium (DMEM) Nutrient Mixture F12 containing 10% FBS, and 1% penicillin-streptomycin (Gibco BRL). All cells used in the experiments were between passages 3 and 10. The experiments were performed after the cells reached confluence.

2.3. Preparation of FA/albumin complex

The method we developed to solubilize VLCFAs in aqueous medium is based on the formation of an FA/albumin complex in the presence of a small amount of isopropanol (IP; FA/IP/BSA) [52]. Briefly, 300 nmol of FA dissolved in 50 μL IP was warmed to 37 °C, while 6.6 mg of BSA was dissolved in 2 mL of culture medium at 37 °C. The preparations were combined and mixed by water sonication at 150 W for 1–5 min at 37 °C. The resulting solution containing the complex was further incubated in a water bath at 37 °C for 60 min. The molar ratio of FA/BSA was 3:1 and the maximum concentration of IP in the culture medium was 0.5% (v/v). The solubility of VLCFAs in the FA/IP/BSA method was compared to that in the conventional method using FA, NaOH (Na), and BSA (FA/Na/BSA). For this, 300 nmol of FA in 50 μL IP was transferred to a glass tube. After evaporation under N_2 flow, 100 μL of 100 mM NaOH was added, followed by heating at 65 °C in a water bath for 5 min, while 6.6 mg of BSA was dissolved in 1.9 mL of culture medium at 37 °C. These preparations were thoroughly mixed by sonication as described above. The molar ratio of FA/NaOH/BSA was 3:6:1. The resulting FA solutions were filtered through a 0.22 μm filter. The filtrates were subjected to lipid extraction and methanolysis to determine the amount of FA using gas chromatography (GC), as described below.

2.4. FA uptake assay

CHO, IFRS1, and PC12 cells were each seeded at 1×10^6 cells per dish in 100-mm petri dishes with 10 mL of FBS-containing medium for 24 h at 37 °C in a CO_2 incubator. The culture medium was replaced with 10 mL serum-free medium for 24 h, followed by treatment with VLCFAs (C20:0, C20:1, C22:0, C22:1, C23:0, C24:0, C24:1, C25:0, and C26:0 FA) or LCFAs (C16:0, C18:0, and C18:1 FA) as FA/BSA complexes prepared according to the FA/IP/BSA method. After 24 h of incubation, the conditioned medium was removed, and the cells were washed with 2 mL of FBS-free medium containing 1% BSA. The conditioned medium and medium containing BSA used for washing were combined and subjected to lipid extraction. The added FA in this combined solution represented FA remaining in the medium. The added FA detected in the extract of the harvested cells represented FA taken up by the cells. Lipids obtained from the medium or harvested cells were extracted as previously described [55] after addition of a known amount of synthetic DAPC or 17:0/17:0 PC as an internal standard. Aliquots of the lipid extract were treated with 5% HCl-methanol at 100 °C for 60 min to prepare fatty acid methyl esters (FAMEs). FAMEs were purified by TLC with a developing solvent system of petroleum ether/diethyl ether/acetic acid (80:20:1, v/v/v) and analyzed by GC using

a capillary column (DB-225, 0.25 μm film thickness, 30 m length, 0.25 mm ID; Agilent Technologies, Santa Clara, CA, USA). The oven temperature was maintained at 100 °C for 0.5 min and raised to 195 °C at a rate of 25 °C/min. It was then increased to 205 °C at a rate of 3 °C/min, followed by 240 °C at 8 °C/min, and maintained constant for 10 min. The oven temperature was then decreased to 100 °C before the injection of the next sample. The amount of each FA was calculated based on the ratio of the peak area between the target peak and the peak of 17:0 from 17:0/17:0 PC or 20:0 from 20:0/20:0 PC as the internal standard.

For the treatment with TDYA peroxisome inhibitor plus FA, CHO-K1 cells were seeded at a density of 1×10^6 cells in 100-mm petri dishes with 10 mL of FBS-containing medium for 24 h at 37 °C in the CO_2 incubator. The culture medium was replaced with 10 mL serum-free medium for 24 h, followed by pretreatment with 30 μM TDYA. Following incubation for 6 h, FA was added and the cells were incubated for 24 h in the presence or absence of TDYA. After the incubation period, lipids in the cells and medium were extracted separately as previously described [55] after addition of the appropriate internal standard as described above. The samples were subjected to methanolysis for determination of the FA by GC as described above.

2.5. Cytotoxicity assay

CHO, PC12, or IFRS1 cells were seeded in 35-mm dishes at 2×10^5 cells/dish at 37 °C in a CO_2 incubator. Following incubation for 24 h, the culture medium was replaced with fresh serum-free medium and supplemented with different concentrations of FA as the FA/BSA complex prepared using the FA/IP/BSA method. Control cells were treated only with the vehicle (BSA + IP). After 48 h of supplementation, adherent cells were harvested with the aid of trypsin/EDTA, washed with PBS, and subjected to a trypan blue dye exclusion assay to assess the number of living cells. The results were calculated as a percentage of vehicle-treated control cells.

For TDYA plus FA treatment, CHO-K1 cells were seeded onto 35-mm dishes at a density of 2×10^5 cells/dish at 37 °C in the CO_2 incubator for 24 h. The culture medium was replaced with fresh serum-free medium and the cells were incubated for 24 h. Subsequently, the cells were incubated with 30 μM TDYA before the addition of FA. After incubation for 6 h, FA was added for 48 h in the presence or absence of TDYA. After incubation, the cells were fixed for fluorescence microscopy, as described below.

2.6. Ultraviolet (UV)- and staurosporine-induced apoptosis in CHO cells

CHO cells were seeded onto 35-mm dishes at a density of 2×10^5 cells/dish at 37 °C in the CO_2 incubator. Following incubation for 24 h, the culture medium was replaced with serum-free medium, and the cells were exposed to UV irradiation at doses of 5, 10, and 20 mJ/cm^2. After 6 h of incubation, adherent cells were harvested using trypsin/EDTA, washed with PBS, and stained with trypan blue. Cells that excluded the stain were considered viable.

CHO cells were seeded onto 35-mm dishes at a density of 2×10^5 cells/dish at 37 °C in the CO_2 incubator. Following incubation for 24 h, the culture medium was replaced with serum-free medium and supplemented with different concentrations of staurosporine. After 6 h of supplementation, adherent cells were harvested with the aid of trypsin/EDTA, washed with PBS, and subjected to the aforementioned trypan blue dye exclusion test to assess the number of living cells.

2.7. Nuclear staining with DAPI (4',6'-Diamidino-2-phenylindole)

CHO or PC12 cells were seeded onto 35-mm dishes at a density of 2×10^5 cells/dish for 24 h. The medium was replaced with serum-free medium and the cells were incubated with FA at the indicated concentrations for 48 h in the presence or absence of TDYA. FA-treated and untreated cells were fixed with 4% paraformaldehyde in PBS for 20 min at 37 °C, permeabilized with 0.1% Triton X-100 in PBS for 5 min at 37 °C, and washed using PBS. The cells were incubated with DAPI (10 μg/mL) at 37 °C for 30 min, washed with PBS, and observed immediately by fluorescence microscopy. Condensed or fragmented nuclei were indicative of apoptotic cells, while intact nuclei indicated viable cells. The numbers of total and apoptotic cells in each microscopic field were counted and the percentage of living cells was calculated.

2.8. DNA fragmentation assay

CHO or PC12 cells were seeded onto 35-mm dishes at a density of 2×10^5 cells/dish for 24 h. The medium was replaced with serum-free medium and the cells were incubated with FA at the indicated concentrations for 48 h. The medium and adherent cells were collected and centrifuged at 2,100 rpm for 5 min at 4 °C. The supernatant was gently withdrawn, and the resultant pellet was lysed in 341 μL of 100 mM Tris-HCl (pH 8.5) containing 5 mM EDTA, 0.2 M NaCl, 0.2% SDS, and 0.2 mg/mL proteinase K at 37 °C for 60 min. Then, 10 μL of 10 mg/mL proteinase K was added to each sample and allowed to stand for 30 min at 50 °C. Subsequently, 141 μL of 5 M NaCl and 471 μL of ethanol were added to the lysate and kept at -80 °C for 60 min. Following centrifugation for 30 min at 15,000

rpm and 4 °C, the DNA pellets were individually dissolved in 20 μL of 10 mM Tris-HCl (pH 7.2) and 2 μL of RNase at 37 °C for 30 min. The DNA samples were each loaded onto a 1.5% agarose gel, separated by electrophoresis, and analyzed for their extent of fragmentation under UV light.

2.9. Statistical analysis

Statistical analysis was performed by one-way ANOVA with post-hoc Tukey test (to compare more than two groups).

3. Results

3.1. FA/IP/BSA improves solubility of VLCFAs

We recently reported that adding VLCFAs as an IP solution into aqueous BSA under warm conditions (~ 37 °C) facilitate the formation of the FA/albumin complex and that VLCFAs prepared by the FA/IP/BSA method are efficiently taken up by cultured cells [52]. In this study, we applied our method to C16–C26 FAs with saturated or unsaturated carbon chains to evaluate the cytotoxicity of these FAs. As shown in Fig. 1A and C, all saturated and unsaturated FAs prepared as FA/IP/BSA complexes passed through the 0.22 μm filter, indicating that most FAs prepared by this method completely formed albumin complexes. In contrast, saturated FAs prepared by the conventional method using FA, NaOH and albumin (FA/Na/BSA) did not completely form albumin complexes, except for C16:0 FA. This conventional method seems to be applicable to unsaturated VLCFAs, but not saturated FA, especially for C≥20 VLCFAs (Fig. 1B and D). The final IP concentration in the medium did not exceed 0.5% in all experiments. IP up to 2% in the medium did not affect cell viability, as we previously described [52].

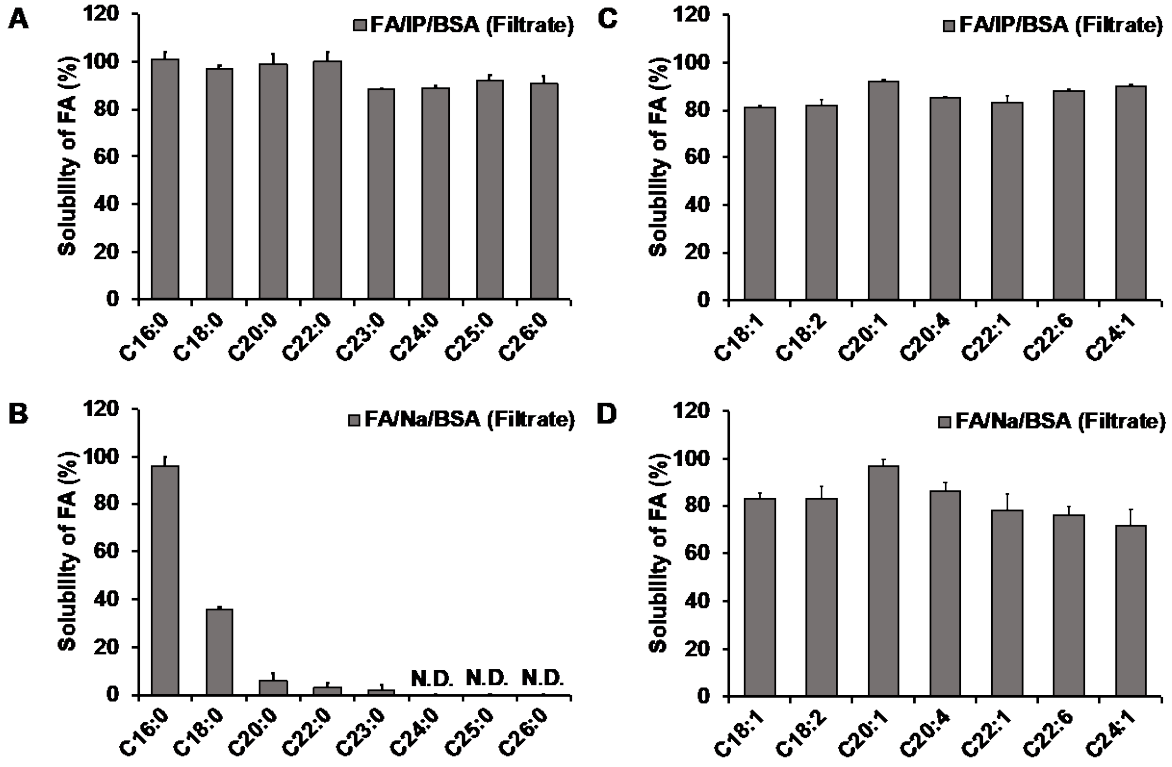

Fig. 1. IP facilitates formation of VLCFA/BSA complexes.

FAs (300 nmol) dissolved in IP were mixed with a BSA solution (FA/IP/BSA) (A, C). FAs (300 nmol) were

treated with NaOH solution followed by heating at 65 °C and mixed with BSA solution (FA/Na/BSA) (B, D). The complexed solutions were filtered through a 0.22 μm membrane filter. FAs dissolved in the filtrate were extracted and subjected to GC analysis after methyl esterification as described in section 2.4. Values represent the mean ± S.D. of three independent experiments. N.D. denotes not detected.

3.2. Uptake of exogenous FAs from culture medium and accumulation of FAs in cellular lipids in CHO cells

We determined the uptake and accumulation levels of saturated (S) or monounsaturated (MU) VLCFAs in peroxisome-deficient (CHO-zp102) and wild-type (CHO-K1) cells using the complexation approach (FA/IP/BSA) [52]. The amounts of FA taken up and accumulated in cells were defined as the decrement of FAs in the culture medium and increment of FA in the cells, respectively (Fig. 2A–D), during the 24 h incubation with 30 μM (300 nmol/dish) FAs in serum-free medium. Most of the FA detected in the cells were not free, but rather were acylated, as we previously described [52].

In wild-type cells, the amounts of VLCFAs (C20:1, C22:0, C22:1, C23:0, C24:0, C24:1, C25:0, and C26:0 FA) taken up by cells were much higher than those of VLCFAs accumulated in the cells (Fig. 2A, C). For example, the amount of C20:1 FA taken up by cells was 250 nmol/dish, whereas the C20:1 FA accumulated in the cells was 35 nmol/dish, indicating that most parts of the C20:1 FA taken up were metabolized during the 24 h incubation in wild-type cells. The findings were in contrast to the result in peroxisome-deficient cells, where the C20:1 FA taken up (230 nmol) was balanced by the accumulation of C20:1 FA in the cells (210 nmol) (Fig. 2D). These results indicate that peroxisomal oxidation seems to operate actively for the clearance of C20:1 FA in wild-type cells. Similar results were observed in experiments with C22:1 and C24:1 FA. Although the uptake capacity of S-VLCFAs (C22:0 to C26:0 FA) in peroxisome-deficient cells was less than that in wild-type cells, the cell uptake of these S-VLCFAs was almost balanced by the accumulation in the cells (Fig. 2B). In contrast, there was a large difference between the uptake and accumulation of these S-VLCFAs in wild-type cells. From these observations, it can be concluded that C20:1, C22:0, C22:1, C23:0, C24:0, C24:1, C25:0, and C26:0 FA are cleared exclusively by peroxisomal oxidation. This conclusion was also supported by the fact that time-dependent accumulations of chain-shortened metabolites of C23:0 FA, such as C19:0 and C17:0 FA, were observed in wild-type cells but not in peroxisome-deficient cells, as reported in our previous study [52].

The uptake of exogenous C16:0 FA from the culture medium was comparable level between wild-type and peroxisome-deficient cells. The cellular levels of C16:0 FA and the FA composition of

cellular lipids were also similar in these cells (Fig. 2A, B). This was also the case for C18:0 FA (Fig. 2A, B). These results indicate that the uptake capacity and metabolic manner of C16:0 and C18:0 FA in peroxisome-deficient cells were similar to those in wild-type cells. Thus, peroxisomal oxidation does not contribute to the clearance of C16:0 and C18:0 FA.

Although the accumulation level of C18:1 FA was higher in peroxisome-deficient cells, the clearance level of C18:1 FA in the peroxisome-deficient cells was comparable to that observed in wild-type cells (~ 100 nmol/dish each; Fig. 2C, D). These results suggest that mitochondria play a pivotal role in the oxidative metabolism of C16:0, C18:0, and C18:1 FA.

The difference between the amount of C20:0 FA uptake by the cells and that of C20:0 FA accumulation in the peroxisome-deficient cells was ~ 50 nmol/dish (Fig. 2B); however, it was 200 nmol in wild-type cells (Fig. 2A). These results indicated that ~ 75% of C20:0 FA that was taken up was cleared by peroxisomal β-oxidation.

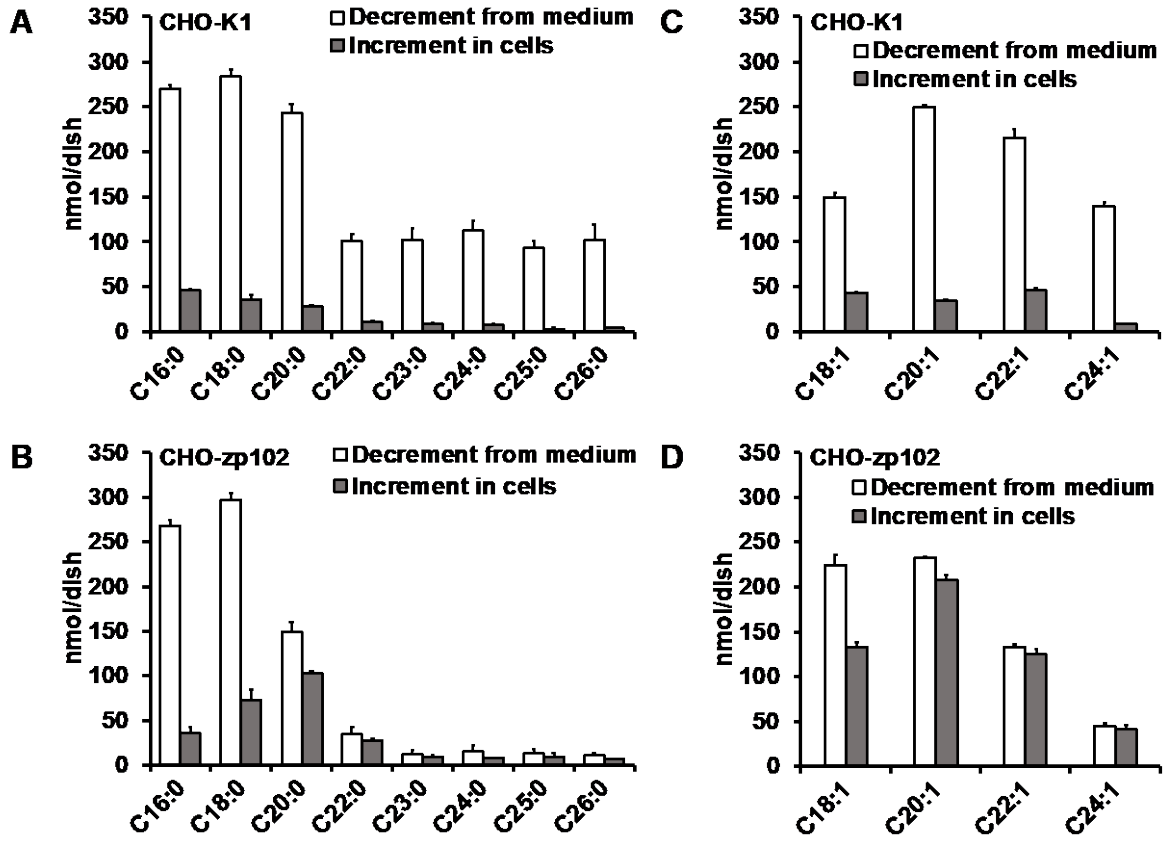

Fig. 2. Cellular uptake of FA in CHO-K1 and CHO-zp102 cells.

CHO-K1 (wild-type) and CHO-zp102 (peroxisome-deficient) cells were incubated with 30 μM of C16:0, C18:0, C18:1, C20:0, C20:1, C22:0, C22:1, C23:0, C24:0, C24:1, C25:0, or C26:0 FA in serum-free medium for 24 h

(A–D). The medium and cells were collected separately after 24 h and subjected to lipid extraction. The fatty acid methyl esters were analyzed by GC, as mentioned in section 2.4. Values represent the mean ± S.D. of three independent experiments.

3.3. Cytotoxicity of extracellular VLCFAs in peroxisome-deficient CHO cells

The effects of VLCFAs on peroxisome-deficient CHO cells were also examined. Cytotoxic effects of C20:0, C20:1, C22:0, C22:1, and C24:1 FA were evident with peroxisome-deficient cells (Fig. 3A). C20:0 FA showed the highest toxicity, which was observed at 5 μM. A common feature of these toxic VLCFAs is that they tended to accumulate in cellular lipids of peroxisome-deficient cells (Fig. 2). In contrast, C16:0, C18:0, C18:1, C23:0, and C25:0 FA did not promote any loss of cell viability up to 30 μM (Fig. 3A). Interestingly, C24:0 and C26:0 FA slightly enhanced the cell survival of serum-starved peroxisome-deficient cells (Fig. 3A). In contrast to peroxisome-deficient cells, cytotoxic effects were not observed following a 48 h incubation with up to 30 μM of C16:0, C18:0, C18:1, C20:1, C22:0, C22:1, C23:0, C24:1, and C25:0 FA (Fig. 3B). Marked cytotoxic effects were observed only when the wild-type cells were incubated with 30 μM of C20:0 FA. Notably, C24:0 and C26:0 FA in wild-type CHO cells tended to have positive effects on cell survival, which was also observed in peroxisome-deficient cells (Fig. 3B). Wild-type and peroxisome-deficient CHO cells showed similar responses to UV- or staurosporine-induced apoptosis (Supplementary Fig. 1).

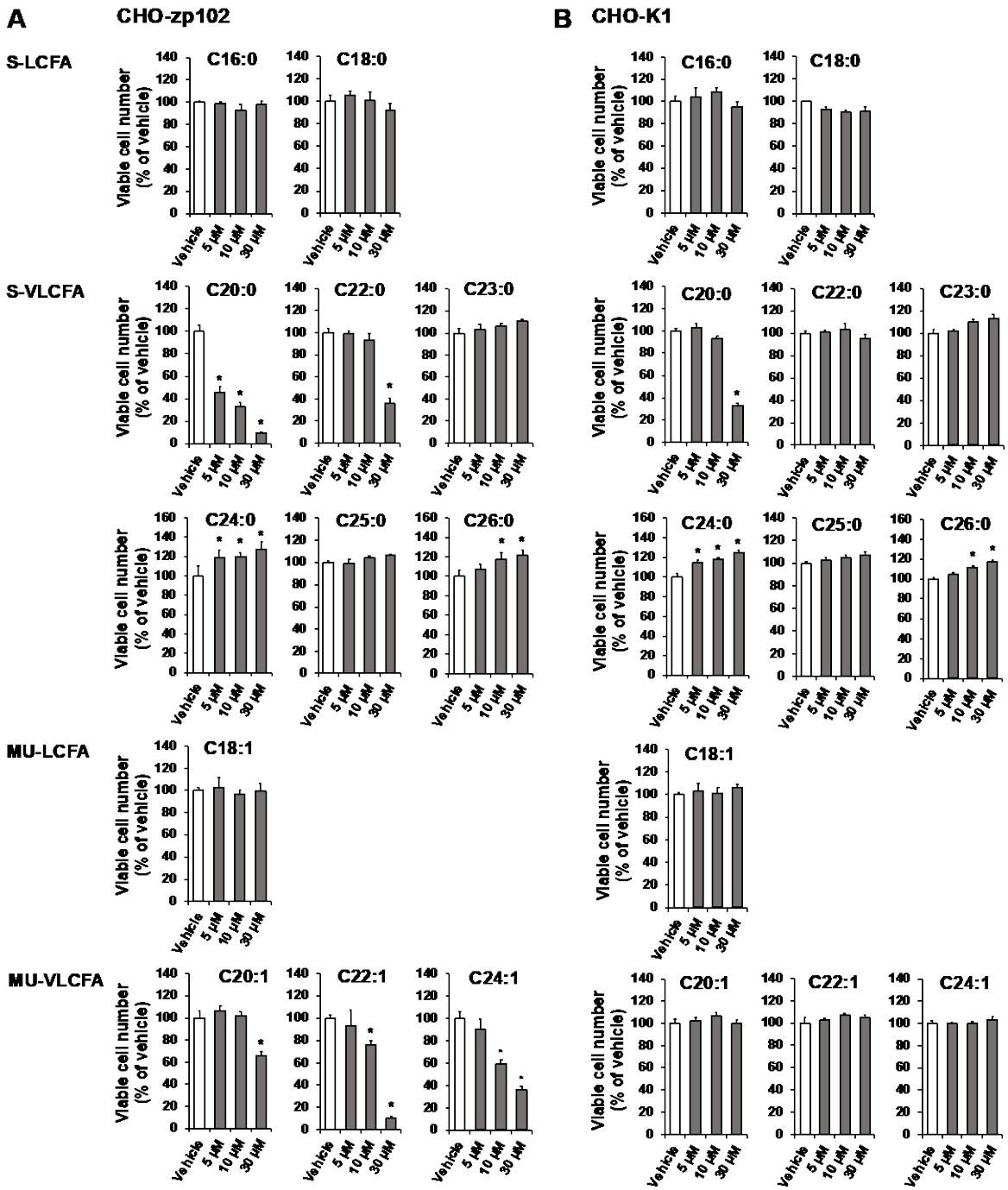

Fig. 3. VLCFAs induce peroxisome-deficient CHO cell death.

CHO-zp102 (peroxisome-deficient) and CHO-K1 (wild-type) cells were incubated in serum-free medium with the indicated concentrations of C16:0, C18:0, C18:1, C20:0, C20:1, C22:0, C22:1, C23:0, C24:0, C24:1, C25:0, or C26:0 FA for 48 h (A, B). Cells were harvested by trypsin-EDTA treatment, and subjected to the trypan blue

dye exclusion test. The data shown are the percentages of the values of the vehicle-treated control cells. Values represent the mean ± S.D. of three independent experiments. Statistical analysis was performed using one-way analysis of variance (ANOVA) followed by Tukey's multiple comparison test. *$p < 0.05$ vs. vehicle.

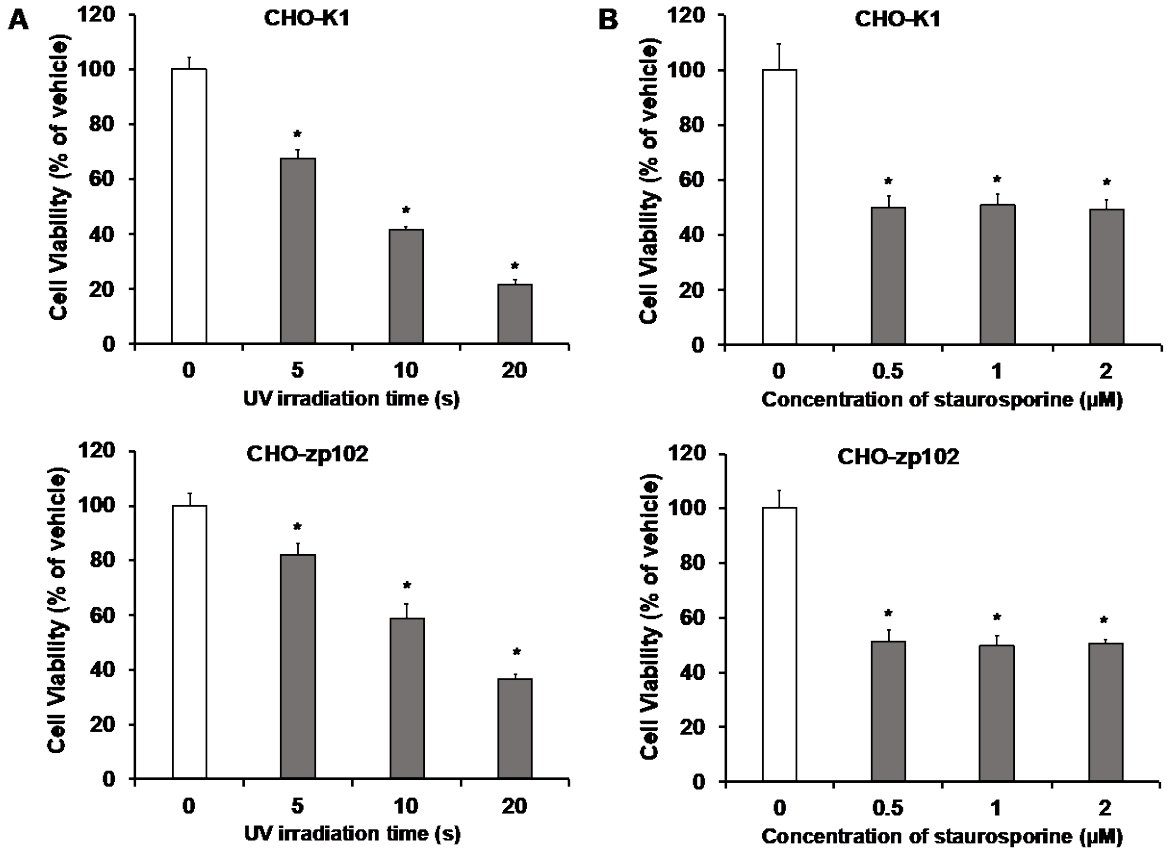

Supplementary Fig. 1. Responses of CHO cells to UV- and staurosporine-induced apoptosis.

CHO-K1 (wild-type) and CHO-zp102 (peroxisome-deficient) cells were irradiated with UV for 5–20 s. Next, the cells were incubated in serum-free medium for 6 h (A). CHO-K1 and CHO-zp102 cells were treated with the indicated concentrations of staurosporine and incubated in serum-free medium for 6 h (B). Living cells were counted using the trypan blue dye exclusion test. Values represent the mean ± S.D. of three independent experiments. Statistical analysis was performed using one-way analysis of variance (ANOVA) followed by Tukey's multiple comparison test. *$p < 0.05$ vs. vehicle.

3.4. VLCFAs induce apoptosis in peroxisome-deficient CHO cells

Nuclear morphology and DNA ladder formation were assessed to clarify whether the observed FA-toxicity resulted in apoptotic cell death. As shown in Fig. 4A, most peroxisome-deficient cells incubated with 30 μM of C20:0, C22:0, C22:1, and C24:1 FA showed morphological alterations of nuclei, such as condensed chromatin and fragmentation. However, most of the control cells did not

display any changes in their nuclei. The living cell ratio was calculated by counting the cells that retained intact nuclei in total cells. The results shown in Fig. 4B are in good agreement with those obtained from the trypan blue dye exclusion assay (Fig. 3). The apoptotic features of peroxisome-deficient cells treated with 30 μM of C20:0, C22:0, C22:1, and C24:1 FA were also confirmed by a DNA fragmentation assay (Fig. 4C). In contrast to VLCFAs, peroxisome-deficient cells treated with 30 μM of C18:1, C24:0, and C26:0 FA did not display apoptotic features, as judged by both nuclear condensation and DNA fragmentation (Fig. 4A–C). C20:0 FA (30 μM)-induced cell death in wild-type cells was also apoptotic, as judged by nuclear shape and DNA fragmentation, in contrast to the treatment with C24:0 FA (Fig. 4D–F).

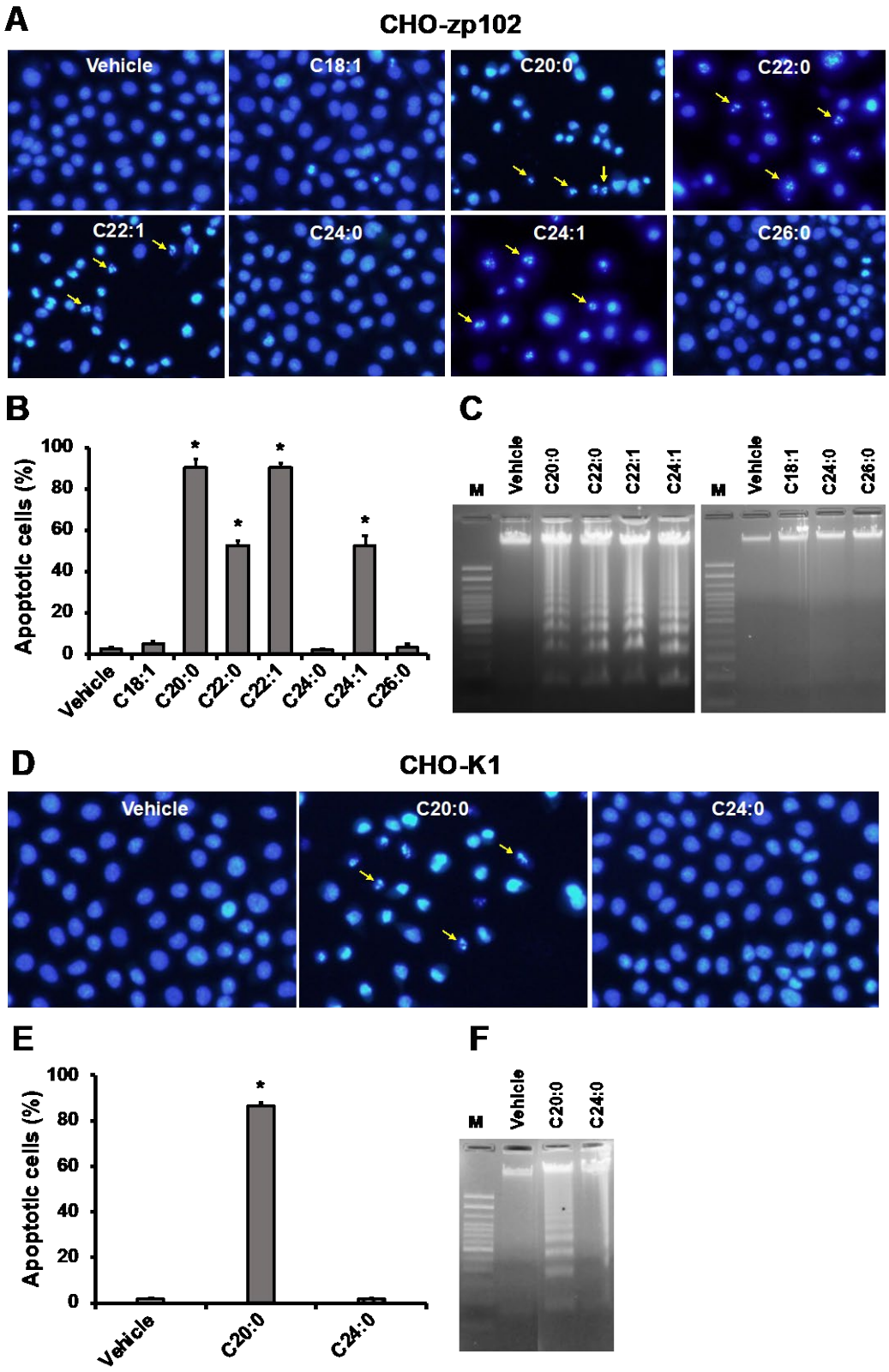
A
CHO-zp102
Vehicle
C18:1
C20:0
C22:0
C22:1
C24:0
C24:1
C26:0
B
Apoptotic cells (%)
100
80
60
40
20
0
Vehicle
C18:1
C20:0
C22:0
C22:1
C24:0
C24:1
C26:0
C
M
Vehicle
C20:0
C22:0
C22:1
C24:1
M
Vehicle
C18:1
C24:0
C26:0
D
CHO-K1
Vehicle
C20:0
C24:0
E
Apoptotic cells (%)
100
80
60
40
20
0
Vehicle
C20:0
C24:0
F
M
Vehicle
C20:0
C24:0

Fig. 4. VLCFAs induce apoptosis in peroxisome-deficient CHO cells.

CHO-zp102 (peroxisome-deficient) and CHO-K1 (wild-type) cells were treated with 30 μM FA in serum-free medium for 48 h, stained with DAPI, and observed by fluorescence microscopy (A, D). The percentage of living cells in each dish was assessed as described in section 2.7 (B, E). Values represent the mean ± S.D. of three independent experiments. Statistical analysis was performed using one-way analysis of variance (ANOVA) followed by Tukey's multiple comparison test. $*p < 0.05$ vs. vehicle. The cells were treated with the indicated concentrations of FA for 48 h and DNA fragmentation was analyzed using 1.5% agarose gel electrophoresis. M indicates the 100-bp DNA ladder size marker (C, F). The data are representatives of three independent experiments.

3.5. Effect of peroxisome inhibitor on the accumulation of C20:0 FA and cytotoxicity

The cytotoxicity of VLCFAs is possibly related to their cellular accumulation, which is prevented by peroxisomal β-oxidation. To obtain further evidence for this hypothesis, we examined whether the peroxisome inhibitor enhances the sensitivity to cytotoxic C20:0 FA by augmenting its accumulation in wild-type cells. TDYA, a potent inhibitor of acyl-CoA oxidase 1, was utilized to inhibit peroxisomal β-oxidation, a peroxisomal function [56]. When wild-type cells were supplemented with 5 and 10 μM C20:0 FA in the absence of TDYA, accumulation of C20:0 FA in the cellular lipids was marginal, with no apparent cytotoxicity (Fig. 5A, B). At 30 μM C20:0 FA, the accumulation of C20:0 FA (28 nmol/dish) became apparent, and notable cytotoxicity was observed (Fig. 5A, B). When TDYA was added to the culture medium, the accumulation of C20:0 FA in cellular lipids in the wild-type CHO cells was significantly enhanced by low concentrations of C20:0 FA (5 μM, 15 nmol/dish; 10 μM, 29 nmol/dish; 30 μM, 64 nmol/dish) (Fig. 5A). The levels of C20:0 FA accumulation in TDYA-treated wild-type cells were comparable to those observed in C20:0 FA accumulation in peroxisome-deficient CHO cells (5 μM, 16 nmol/dish; 10 μM, 44 nmol/dish; 30 μM, 79 nmol/dish) (Fig. 5A), indicating that peroxisomal β-oxidation was inhibited by TDYA. We found that the sensitivity to cytotoxic C20:0 FA was enhanced in TDYA-treated wild-type cells to a similar extent as that observed in peroxisome-deficient cells (Fig. 5B). The relationship between cytotoxicity and cellular accumulation of C20:0 FA in these experiments clearly showed that C20:0 FA-induced cell toxicity correlates with the intracellular accumulation of C20:0 FA (Fig. 5C).

The inhibitory effect of TDYA on the peroxisomal β-oxidation was also confirmed by experiments with C23:0 FA, where the chain-shortened metabolites of C23:0 FA, such as C19:0 and C17:0 FA were completely absent in the C23:0 FA-supplemented wild-type cells in the presence but not in the absence of 30 μM TDYA (Supplementary Fig. 2). Similar experiments were conducted with C22:1

and C24:1 FA. We found that sensitivity to cytotoxic C22:1 and C24:1 FA was also increased in the presence of TDYA, and that the toxicity was partially correlated with the level of intracellular accumulation of these VLCFAs (Supplementary Fig. 3).

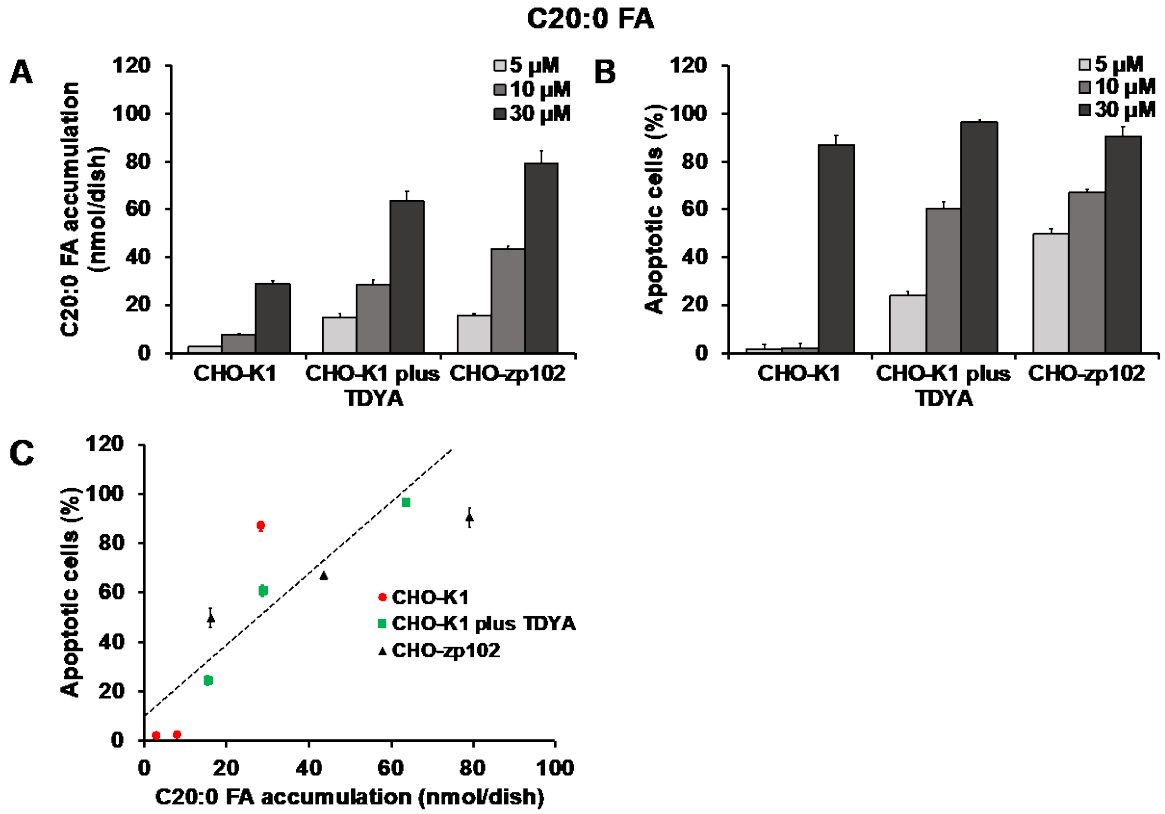

Fig. 5. Correlation between accumulation of C20:0 FA and cellular toxicity.

CHO-K1 (wild-type) or CHO-zp102 (peroxisome-deficient) cells were incubated with the indicated concentrations of C20:0 FA in serum-free medium for 24 h in the absence or presence of 30 μM TDYA. The cells (A) were collected after 24 h and subjected to lipid extraction. The accumulation levels of C20:0 FA in the cells were determined by GC, as mentioned in section 2.4. Values represent the mean ± S.D. of three independent experiments. The percentage of apoptotic cells in each experiment was determined as described in section 2.7. (B). Values represent the mean ± S.D. of three independent experiments. The percentage obtained in the apoptosis assay was plotted against the amount of C20:0 FA accumulated in cellular lipids (C). Values represent the mean ± S.D. of three independent experiments.

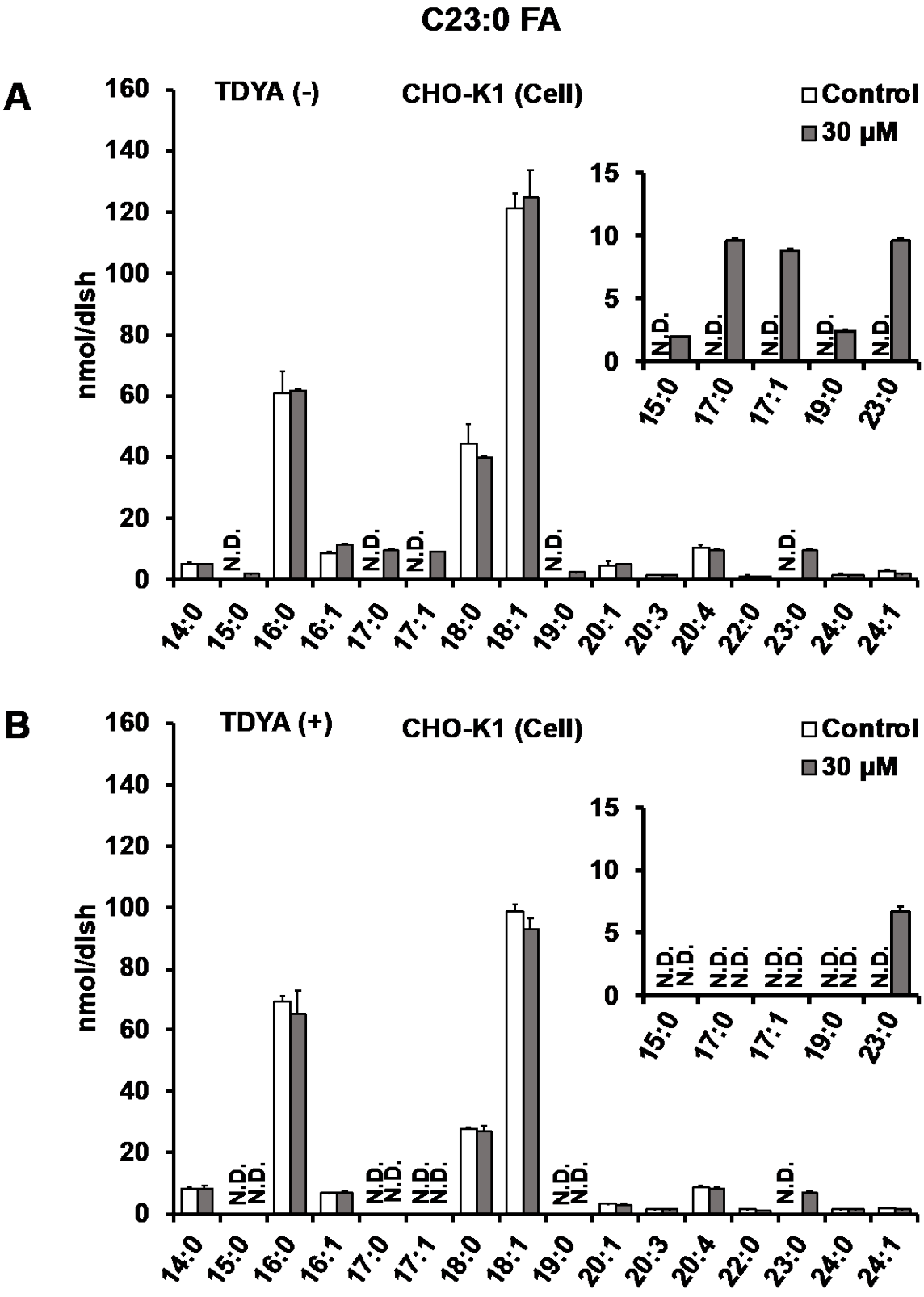
C23:0 FA
A
TDYA (-)
CHO-K1 (Cell)
Control
30 μM
nmol/dlsh
160
140
120
100
80
60
40
20
0
15
10
5
0
N.D.
14:0
15:0
16:0
16:1
17:0
17:1
18:0
18:1
19:0
20:1
20:3
20:4
22:0
23:0
24:0
24:1
B
TDYA (+)
CHO-K1 (Cell)
Control
30 μM

Supplementary Fig. 2. Effect of 10,12-tricosadiynoic acid on C23:0 FA β-oxidation in wild-type CHO cells.

CHO-K1 (wild-type) cells were incubated with the indicated concentrations of C23:0 FA in serum-free medium for 24 h in the presence or absence of TDYA. The cells (A, B) were collected after 24 h and subjected to lipid extraction. The fatty acid methyl esters were analyzed by GC, as mentioned in section 2.4. Values represent the mean ± S.D. of three independent experiments.

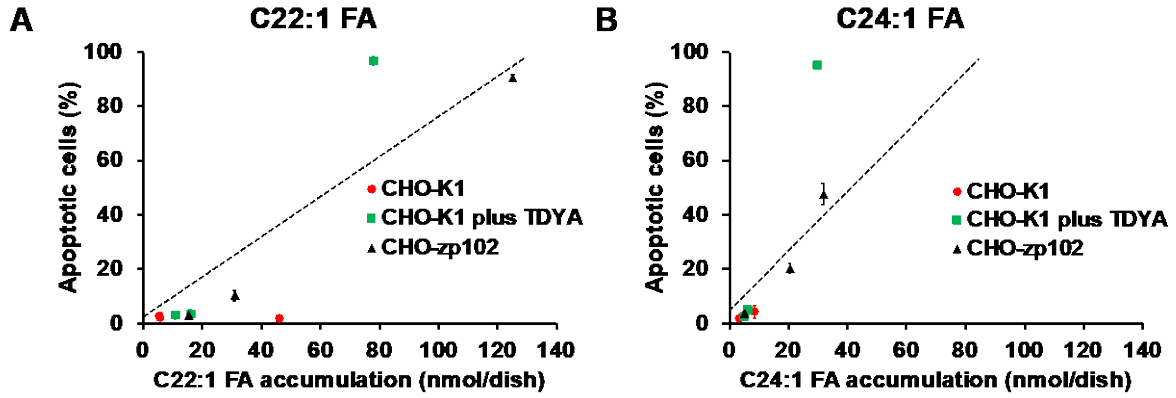

Supplementary Fig. 3. Correlation between accumulation of FA and cellular toxicity.

CHO-K1 (wild-type) or CHO-zp102 (peroxisome-deficient) cells were incubated with different concentrations of C22:1 FA (A) or C24:1 FA (B) in serum-free medium for 24 h in the absence or presence of 30 μM TDYA. The cells were collected after 24 h and subjected to lipid extraction. The accumulation levels of FA and the extent of apoptosis were determined using the same method as mentioned in the legend to Fig. 5. The percentage obtained in the apoptosis assay was plotted against the amount of added FA accumulated in cellular lipids (A, B). Values represent the mean ± S.D. of three independent experiments.

3.6. Cytotoxicity of extracellular VLCFAs in PC12 and FRS1 cells

To determine the effects of VLCFAs in neuronal and myelinating cells, experiments were conducted with PC12 and IFRS1 cells, a neural crest-derived pheochromocytoma cell line, and a Schwann cell-derived cell line, respectively. PC12 cells were sensitive to the cytotoxic effects of C20:0, C22:0, and C24:1 FA. Among these, C20:0 FA showed the highest toxicity and caused a notable increase in cell death at a low concentration (5 μM). We found that C16:0, C18:0, C18:1, C20:1, C22:1, C23:0, C24:0, C25:0, and C26:0 FA did not affect the viability of PC12 cells (Fig. 6A).

We found that treatment with C16:0, C18:0, C18:1, C20:1, C22:0, C22:1, C23:0, C24:0, C24:1, C25:0, and C26:0 FA did not show toxic effects on IFRS1 cells at concentrations of up to 150 μM. A marked decrease in cell viability was observed only when IFRS1 cells were exposed to 150 μM C20:0

FA, which was 30 times higher than that in PC12 cells (Fig. 6B).

A cellular uptake assay was performed in these neuronal cells. When PC12 cells were incubated with 30 μM of C20:0, C22:0, C24:0, and C26:0 FA, the accumulation levels of C20:0, C22:0, C24:0, and C26:0 FA in cellular lipids were 62 nmol/dish, 10 nmol/dish, 5 nmol/dish, 2 nmol/dish, respectively (Fig. 7A). A large amount of accumulation was also observed in the experiment with 150 μM C20:0 FA, but not in those with other VLCFAs, in IFRS1 cells (Fig. 7B). These results are consistent with those observed in CHO cells, in that, VLCFA toxicity correlates with the intracellular accumulation of VLCFAs. Based on observations of their nuclear shape and DNA ladder formation, we confirmed that C20:0 FA-induced cell death of PC12 cells was due to apoptosis (Fig. 7C, D). IFRS1 cells may have a larger capacity for the oxidative activity of peroxisomes. This is because a large amount of exogeneous C20:0 FA is necessary to induce the accumulation of C20:0 FA at toxic levels in IFRS1 cells. The amount of C20:0 FA cleared in IFRS1 cells at 150 μM was twice that cleared in CHO-K1 cells at 30 μM (Supplementary Fig. 4).

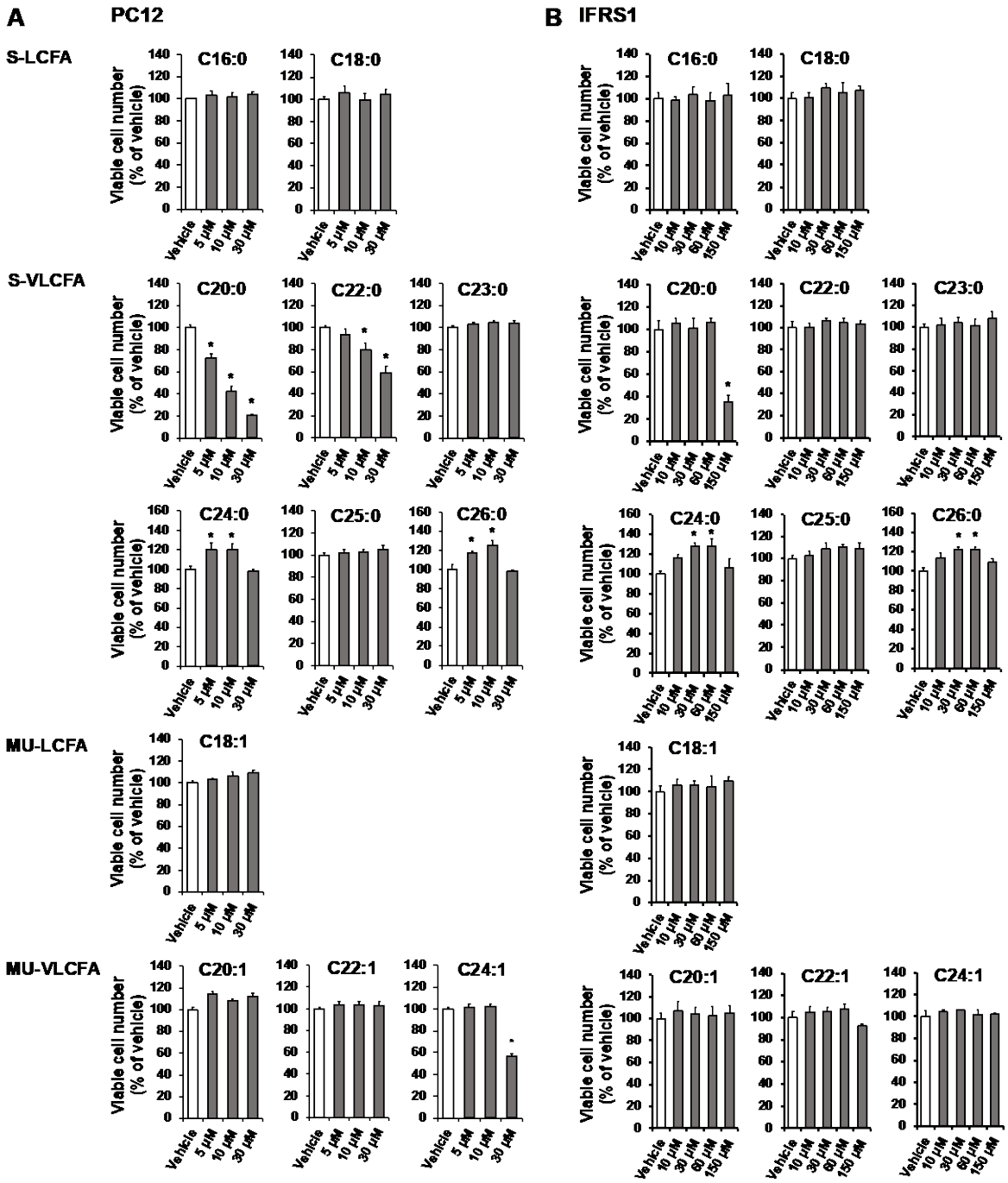

Fig. 6. VLCFAs induces PC12 and IFRS1 cell death.

PC12 (A) or IFRS1 cells (B) were incubated in serum-free medium with the indicated concentrations of C16:0, C18:0, C18:1, C20:0, C20:1, C22:0, C22:1, C23:0, C24:0, C24:1, C25:0, or C26:0 FA for 48 h. Cells were harvested by trypsin-EDTA treatment and subjected to the Trypan blue-exclusion test. The data shown are the

percentages of the values of the vehicle-treated control cells. Values represent the mean ± S.D. of three independent experiments. Statistical analysis was performed using one-way analysis of variance (ANOVA) followed by Tukey's multiple comparison test. *$p < 0.05$ vs. vehicle.

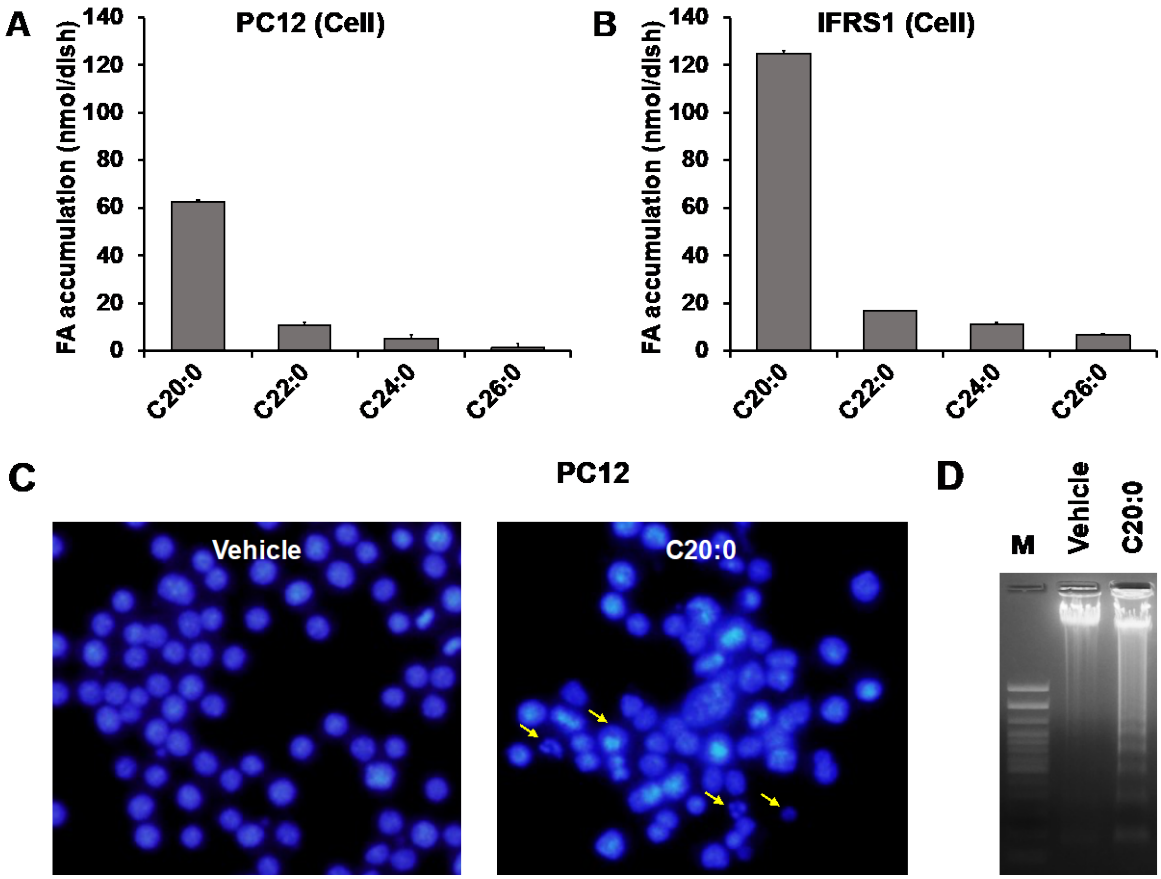

Fig. 7. Cellular accumulation of VLCFAs in PC12 and IFRS1 cells.

PC12 cells (A) were incubated with 30 μM of C20:0, C22:0, C24:0, or C26:0 FA in serum-free medium for 24 h. IFRS1 cells (B) were incubated with 150 μM of C20:0, C22:0, C24:0, or C26:0 FA in serum-free medium for 24 h. Cells were collected at the specific time points and subjected to lipid extraction. The fatty acid methyl esters were analyzed by GC to determine the added FA accumulated in the cellular lipids, as mentioned in section 2.4. Values represent the mean ± S.D. of three independent experiments. PC12 cells were treated with 30 μM C20:0 FA in serum-free medium for 48 h, stained with DAPI, and observed by fluorescence microscopy (C). The cells were treated with the indicated concentrations of FA for 48 h, and DNA fragmentation was analysed using 1.5% agarose gel electrophoresis. M indicates the 100-bp DNA ladder size marker (D). The data are representative of three independent experiments.

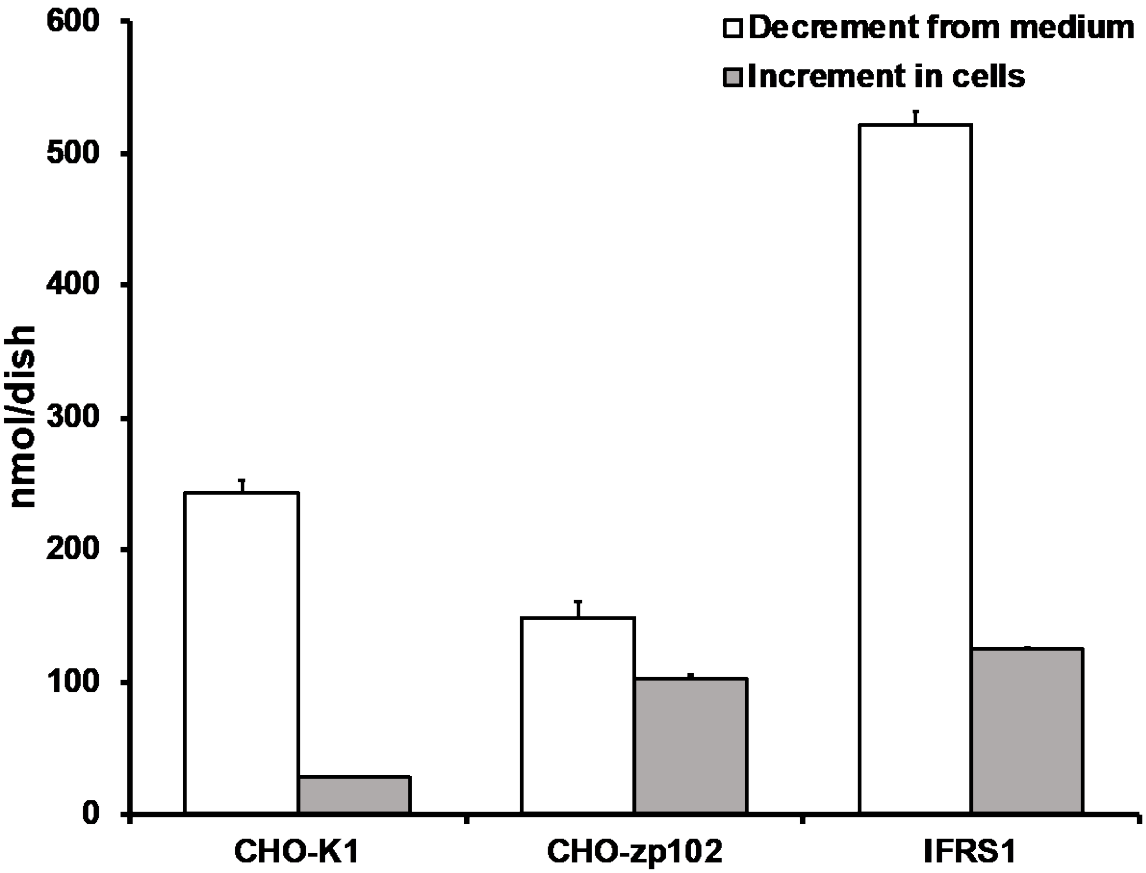

Supplementary Fig. 4. Cellular uptake of C20:0 FA by CHO and IFRS1 cells.

CHO and IFRS1 cells were incubated with 30 μM and 150 μM C20:0 FA, respectively, in serum-free medium for 24 h. The medium and cells were collected separately after 24 h and subjected to lipid extraction. The fatty acid methyl esters were analyzed by GC, as mentioned in section 2.4. Values represent the mean ± S.D. of three independent experiments.

4. Discussion

ALD is the most frequent peroxisomal disease caused by mutations in the *ABCD1* gene, which is responsible for the introduction of VLCFAs into the peroxisome [14–20]. The inability to oxidize VLCFAs in peroxisomes results in the abnormal accumulation of S-VLCFAs, such as C24:0 and C26:0 FA, in the patient's body [21–36]. Abnormal accumulation of S-VLCFAs is believed to cause ALD symptoms, including demyelination of nervous tissues and adrenal insufficiency [37–41]. However, the severity of symptoms and the extent of accumulation of these S-VLCFAs in the plasma are not clearly correlated, and the mechanisms of tissue degeneration are largely unknown.

One of the difficulties in studying the effect of VLCFAs is that they cannot dissolve in aqueous medium. S-VLCFAs are extremely hydrophobic, and thus are not efficiently delivered to cells. Recently, we developed a method to disperse VLCFAs in an aqueous medium using a small amount of IP in the presence of BSA under warm conditions (37 °C) [52]. VLCFAs were efficiently introduced into the cells [52]. Here, we confirmed that our method can be applied to C26:0 FA. We also showed the limitation of the conventional method, in which FA is converted to an albumin complex after dissolving it into its sodium salt (FA/Na/BSA). The FA/Na/BSA method was applicable to MU-VLCFAs and saturated FA up to C16, but not to saturated FA above C18.

Using this method, we characterized the oxidative metabolism of LCFAs and VLCFAs of different chain lengths (Fig. 2). The characterization was based on the clearance level of the added FA during the incubation, which was calculated as the difference between the amount of FA that disappeared from the medium and that appearing in the cellular lipids in CHO cells (medium-cellular lipids [M-C] value). In the case of C16:0 and C18:0 FA, the M-C values were similarly higher (>200 nmol) in both peroxisome-deficient cells and wild-type cells. Thus, the major oxidative clearance of these LCFAs in both cell types was via mitochondrial activity. This is consistent with earlier reports showing that 94% of the oxidative metabolism of C16:0 FA is performed by mitochondria [57,58].

In the case of FA with chain lengths above C22:0, the M-C values were extremely low (<5 nmol) in peroxisome-deficient cells. In contrast, the corresponding M-C values in wild-type cells were considerably higher (>100 nmol), suggesting peroxisome-dependent clearance of these VLCFAs in wild-type cells. Thus, these VLCFAs are regarded as peroxisomal substrates. This conclusion is the same as that in our previous study showing that time-dependent accumulation of chain-shortened metabolites of C23:0 FA, such as C19:0 and C17:0 FA, was observed in wild-type cells but not in peroxisome-deficient cells [52], which is consistent with previous reports [59–65]. The oxidative clearance of S-VLCFAs in peroxisomes may be a driving force for continuous uptake into the cells

and could explain the large difference between the decrements of S-VLCFAs from the medium of wild-type cells and those from medium of peroxisome-deficient cells. The oxidative clearance rate also could explain the difference between the decrease in C20:0 FA and that of C22:0–C26:0 FA from the medium in these types of CHO cells.

Based on the comparison of M-C values of C20:0 FA in wild-type and peroxisome-deficient cells, we observed that 75% of oxidative metabolism of C20:0 FA was performed by peroxisomes in wild-type cells. The shorter chain length limit of VLCFAs that are preferentially oxidized in peroxisomes differs among studies (C22 in some studies, C20 in others) [66,67]. Our results indicated that C20:0 FA is a good peroxisome substrate.

The metabolism of MU-VLCFAs seemed to be different from that of S-VLCFAs in terms of the acylation capacity of cellular lipids. Accumulation of C20:1, C22:1, and C24:1 FA was evident in peroxisome-deficient cells, indicating that MU-VLCFAs are metabolized differently from S-VLCFAs in peroxisome-deficient cells.

In this study, we found that C20:0 FA exerted the strongest toxic effect among the C16–C26 FAs tested. The toxicity of C20:0 FA was observed at 5 μM in the peroxisome-deficient cells and at 30 μM in the wild-type cells, suggesting that the peroxisome-deficient cells are sensitive to the toxicity of C20:0 FA. We also found that C20:1, C22:0, C22:1, and C24:1 FA were toxic to the peroxisome-deficient cells at 30 μM, but not to the wild-type cells at this concentration. These data are consistent with earlier studies showing that C20:0 FA (500 μM) was most toxic compared to polyunsaturated FAs and other saturated FAs [68]. Here, we demonstrated that VLCFA-loaded cells undergo apoptosis, with a close correlation between the cytotoxicity and accumulation levels of these VLCFAs in cellular lipids. These observations indicate that the increased sensitivity to VLCFAs toxicity in peroxisome-deficient cells is attributable to the inability of peroxisomes to oxidize these VLCFAs. This notion is supported by the fact that the apoptotic sensitivity of wild-type cells increased in parallel with the accumulation of these VLCFAs when peroxisomal β-oxidation was inhibited by TDYA. Wild-type and peroxisome-deficient CHO cells showed similar responses to UV- or staurosporine-induced apoptosis (Supplementary Fig. 1). From these results, it can be concluded that peroxisomes are crucial organelles for the detoxification of cytotoxic VLCFAs.

Accumulation of S-VLCFAs, such as C24:0 and C26:0 FA, is a useful biomarker for the diagnosis of peroxisome disease and is considered to be involved in symptoms of the disease, such as demyelination. Many reports have described the cytotoxicity of these VLCFAs by induction of necrotic cell death due to increased production of reactive oxygen species (ROS) or impaired

mitochondrial and lysosomal function [42–51]. However, we did not observe cytotoxicity by up to 30 μM of C24:0 and C26:0 FA in the peroxisome-deficient cells; rather, they exhibited cytoprotective action in both the peroxisome-deficient cells and wild-type cells. One of the reasons for this discrepancy may be the difference in the method of delivery of S-VLCFAs into the cells. The FA-dissolving methods used in other investigations involve FA/Na/BSA or FA/cyclodextrin complexes, which do not efficiently dissolve VLCFAs in aqueous medium, as shown here and in our previous study [52]. The resulting VLCFA aggregates may affect the integrity of cellular functions. Ceramides with different *N*-acyl chains perform different functions in cells [69]. Alteration of ceramide composition in cells by overexpression or silencing of ceramide synthases shows that C16:0 ceramide is pro-apoptotic, whereas ceramide with C24:0 is anti-apoptotic [69]. The change in the composition of ceramide species may affect the apoptotic tendency of C24:0- and C26:0-replete cells. Further studies are needed to clarify the effect of the accumulation of C24:0 and C26:0 FA in peroxisome-deficient oligodendrocytes and Schwann cells to better understand peroxisome diseases.

In this study, ≥10 μM C24:1 FA was toxic to peroxisome-deficient cells, whereas the same concentrations of C24:0 FA were not. This is in contrast to the notion that S-VLCFAs are more toxic than the corresponding MU-VLCFAs [70,71]. This discrepancy is attributable to the difference in the accumulation levels of VLCFAs in cells. Here, extensive accumulation of C24:1 FA was achieved using our solubilization technique, whereas C24:0 FA hardly accumulated in the peroxisome-deficient cells, possibly due to halted uptake. Thus, our results do not indicate MU-VLCFAs are more toxic than S-VLCFAs at similar accumulation levels in cells.

In this study, we showed that peroxisome-deficient CHO cells exhibited increased sensitivity to C20:0, C20:1, C22:0, C22:1, and C24:1 FA. This increased sensitivity was caused by the accumulation of VLCFAs in cells whose peroxisomal β-oxidation system was impaired. C20:0 FA was toxic to myelinating cells, PC12 and IFRS1 cells. To the best of our knowledge, there is no report demonstrating the accumulation of C20:0 FA in the plasma or tissues of patients with peroxisome disease. Thus, it is uncertain whether accumulated C20:0 FA exert deteriorating effects in patients with peroxisome diseases, including ALD. However, it should be considered that biosynthesis of VLCFAs is enhanced during the myelination process [72–74]. Patients afflicted by peroxisome disease with an inability to oxidize VLCFAs may become vulnerable when the myelinating cells perform enhanced synthesis of VLCFAs due to the lack of a detoxification device.

Finally, the limitations of this study must be mentioned. Here, we showed the apoptosis-inducing properties (i.e. C20:0, C22:0, C20:1, C22:1, and C24:1 FA) and anti-apoptotic properties (i.e. C24:0

and C26:0 FA) of VLCFAs. These effects were demonstrated in cultured cell systems by introducing high concentrations of VLCFAs solubilized as albumin complexes using our technique. This differs from conditions in patients. For example, the concentration of free C26:0 FA in the blood of patients with ALD is <3 μM [32], and C20:0 FA scarcely accumulates in patients with peroxisome disease. Additionally, most VLCFAs are likely to be produced by endogenous biosynthesis in a controlled manner. The intracellular distribution and accumulation level of VLCFAs may be different in cases where VLCFAs are supplied exogenously and are provided endogenously. Therefore, transiently accumulated VLCFAs may affect cellular events differently from chronically accumulated VLCFAs. This difference should be considered when applying our results to the neurodegeneration of patients with peroxisome disease.

In summary, we found that peroxisomes attenuate cytotoxicity of VLCFAs. Further research is needed to examine whether VLCFA-evoked changes in apoptotic tendency in cells are involved in tissue degeneration in patients with peroxisome disease.

Acknowledgments/grant support

This study was partly supported by the Kobayashi Foundation (to T.T.), Ito Tokuzo Himashi Kenkyu Kikin (to T.T.), and JSPS KAKENHI (Grant Number 19K05863 to T.T.).

References

[1] M. Schrader, H.D. Fahimi, The peroxisome: still a mysterious organelle, Histochem. Cell Biol. 129 (2008) 421–440, https://doi.org/10.1007/s00418-008-0396-9.

[2] R.J. Wanders, H.R. Waterham, Biochemistry of mammalian peroxisomes revisited, Annu. Rev. Biochem. 75 (2006) 295–332, https://doi.org/10.1146/annurev.biochem.74.082803.133329.

[3] M. Schrader, H.D. Fahimi, Mammalian peroxisomes and reactive oxygen species, Histochem. Cell Biol. 122 (2004) 383–393. https://doi.org/10.1007/s00418-004-0673-1.

[4] S.D. Nguyen, M. Baes, P.P. Van Veldhoven, Degradation of very long chain dicarboxylic polyunsaturated fatty acids in mouse hepatocytes, a peroxisomal process, Biochim. Biophys. Acta 1781 (2008) 400–405, https://doi.org/10.1016/j.bbalip.2008.06.004.

[5] H.R. Waterham, M.S. Ebberink, Genetics and molecular basis of human peroxisome biogenesis disorders, Biochim. Biophys. Acta 1822 (2012) 1430–1441, https://doi.org/10.1016/j.bbadis.2012.04.006.

[6] C. Argyriou, M.D. D'Agostino, N. Braverman, Peroxisome biogenesis disorders, Transl. Sci. Rare Dis. 1 (2016) 111–144, https://doi.org/10.3233/TRD-160003.

[7] P.P.V. Veldhoven, Biochemistry and genetics of inherited disorders of peroxisomal fatty acid metabolism, J. Lipid Res. 51 (2010) 2863–2895, https://doi.org/10.1194/jlr.R005959.

[8] J. Berger, F. Dorninger, S. Forss-Petter, M. Kunze, Peroxisomes in brain development and function, Biochim. Biophys. Acta 1863 (2016) 934–955, https://doi.org/10.1016/j.bbamcr.2015.12.005.

[9] S.J. Steinberg, G. Dodt, G.V. Raymond, N.E. Braverman, A.B. Moser, H.W. Moser, Peroxisome biogenesis disorders, Biochim. Biophys. Acta 1763 (2006) 1733–1748, https://doi.org/10.1016/j.bbamcr.2006.09.010.

[10] M. Depreter, M. Espeel, F. Roels, Human peroxisomal disorders, Microsc. Res. Tech. 61 (2003) 203–223, https://doi.org/10.1002/jemt.10330.

[11] K. Hama, T. Nagai, C. Nishizawa C, K. Ikeda, M. Morita, N. Satoh, H. Nakanishi, T. Imanaka, N. Shimozawa, R. Taguchi, K. Inoue, K. Yokoyama, Molecular species of phospholipids with very long chain fatty acids in skin fibroblasts of Zellweger syndrome, Lipids 48 (2013) 1253–1267, https://doi.org/10.1007/s11745-013-3848-5.

[12] Y. Abe, M. Honsho, H. Nakanishi, R. Taguchi, Y. Fujiki, Very-long-chain polyunsaturated fatty acids accumulate in phosphatidylcholine of fibroblasts from patients with Zellweger syndrome

and acyl-CoA oxidase 1 deficiency, Biochim. Biophys. Acta 1841 (2014) 610–619, https://doi.org/10.1016/j.bbalip.2014.01.001.

[13] H. Rosewich, H.R. Waterham, R.J. Wanders, S. Ferdinandusse, M. Henneke, D. Hunneman, J. Gärtner, Pitfall in metabolic screening in a patient with fatal peroxisomal beta-oxidation defect, Neuropediatrics 37 (2006) 95–98, https://doi.org/10.1055/s-2006-923943.

[14] M. Morita, N. Shimozawa, Y. Kashiwayama, Y. Suzuki, T. Imanaka, ABC subfamily D proteins and very long chain fatty acid metabolism as novel targets in adrenoleukodystrophy, Curr. Drug Targets 12 (2011) 694–706, https://doi.org/10.2174/138945011795378577.

[15] J. Mosser, A.M. Douar, C.O. Sarde, P. Kioschis, R. Feil, H. Moser, A.M. Poustka, J.L. Mandel, P. Aubourg, Putative X-linked adrenoleukodystrophy gene shares unexpected homology with ABC transporters, Nature 361(1993) 726–730, https://doi.org/10.1038/361726a0.

[16] S. Kemp, F.L. Theodoulou, R.J. Wanders, Mammalian peroxisomal ABC transporters: from endogenous substrates to pathology and clinical significance, Br. J. Pharmacol. 164 (2011) 1753–1766, https://doi.org/10.1111/j.1476-5381.2011.01435.x.

[17] R.J.A. Wanders, W.F. Visser, C.W. van Roermund, S. Kemp, H.R. Waterham, The peroxisomal ABC transporter family, Pflugers Arch. 453 (2006) 719–734, https://doi.org/10.1007/s00424-006-0142-x.

[18] C. Wiesinger, M. Kunze, G. Regelsberger, S. Forss-Petter, J. Berger, Impaired very long-chain acyl-CoA β-oxidation in human X-linked adrenoleukodystrophy fibroblasts is a direct consequence of ABCD1 transporter dysfunction, J. Biol. Chem. 288 (2013) 19269–19279, https://doi.org/10.1074/jbc.M112.445445.

[19] J. Berger, S. Forss-Petter, F.S. Eichler, Pathophysiology of X-linked adrenoleukodystrophy, Biochimie. 98 (2014) 135–142, https://doi.org/10.1016/j.biochi.2013.11.023.

[20] A.B. Moser, R.O. Jones, W.C. Hubbard, S. Tortorelli, J.J. Orsini, M. Caggana, B.H. Vogel, G.V. Raymond, Newborn screening for X-linked adrenoleukodystrophy, Int. J. Neonatal. Screen. 2 (2016) 15, https://doi.org/10.3390/ijns2040015.

[21] S. Kemp, R. Wanders, Biochemical aspects of X-linked adrenoleukodystrophy, Brain Pathol. 20 (2010) 831–837, https://doi.org/10.1111/j.1750-3639.2010.00391.x.

[22] S. Kemp, J. Berger, P. Aubourg, X-linked adrenoleukodystrophy: Clinical, metabolic, genetic and pathophysiological aspects, Biochim. Biophys. Acta 1822 (2012) 1465–1474, https://doi.org/10.1016/j.bbadis.2012.03.012.

[23] M.C. McGuinness, J.F. Lu, H.P. Zhang, G.X. Dong, A.K. Heinzer, P.A. Watkins, J. Powers, K.D. Smith, Role of ALDP (ABCD1) and mitochondria in X-linked adrenoleukodystrophy, Mol. Cell Biol. 23 (2003) 744–753, https://doi.org/10.1128/MCB.23.2.744-753.2003.

[24] H.W. Moser, K.D. Smith, P.A. Watkins, J. Powers, A.B. Moser, X-linked adrenoleukodystrophy, The Metabolic and Molecular Bases of Inherited Disease, McGraw Hill, New York, 2001, pp. 3257–3301.

[25] H.W. Moser, A.B. Moser, K.K. Frayer, W. Chen, J.D. Schulman, B.P. O'Neill, Y. Kishimoto, Adrenoleukodystrophy: increased plasma content of saturated very long chain fatty acids, Neurology 31 (1981) 1241–1249, https://doi.org/10.1212/wnl.31.10.1241.

[26] I. Singh, A.E. Moser, H.W. Moser, Y. Kishimoto, Adrenoleukodystrophy: impaired oxidation of very long chain fatty acids in white blood cells, cultured skin fibroblasts, and amniocytes, Pediatr. Res. 18 (1984) 286–290, https://doi.org/10.1203/00006450-198403000-00016.

[27] D.K. Lee, N.P. Long, J. Jung, T.J. Kim, E. Na, Y.P. Kang, S.W. Kwon, J. Jang, Integrative lipidomic and transcriptomic analysis of X-linked adrenoleukodystrophy reveals distinct lipidome signatures between adrenomyeloneuropathy and childhood cerebral adrenoleukodystrophy, Biochem. Biophys. Res. Commun. 508 (2019) 563–569, https://doi.org/10.1016/j.bbrc.2018.11.123.

[28] B.J. Pettus, M. Baes, M. Busman, Y.A. Hannun, P.P.V. Veldhoven, Mass spectrometric analysis of ceramide perturbations in brain and fibroblasts of mice and human patients with peroxisomal disorders, Rapid Commun. Mass Spectrom. 18 (2004) 1569–1574, https://doi.org/10.1002/rcm.1520.

[29] Y. Fujiwara, K. Hama, N. Shimozawa, K. Yokoyama, Glycosphingolipids with very long-chain fatty acids accumulate in fibroblasts from adrenoleukodystrophy patients, Int. J. Mol. Sci. 22 (2021) 8645, https://doi.org/10.3390/ijms22168645.

[30] T. Kobayashi, N. Shinnoh, A. Kondo, T. Yamada, Adrenoleukodystrophy protein-deficient mice represent abnormality of very long chain fatty acid metabolism, Biochem. Biophys. Res. Commun. 232 (1997) 631–636, https://doi.org/10.1006/bbrc.1997.6340.

[31] S. Takashima, K. Toyoshi, T. Itoh, N. Kajiwara, A. Honda, A. Ohba, S. Takemoto, S. Yoshida, N. Shimozawa, Detection of unusual very-long-chain fatty acid and ether lipid derivatives in the fibroblasts and plasma of patients with peroxisomal diseases using liquid chromatography-mass spectrometry, Mol. Genet. Metab. 120 (2017) 255–268, https://doi.org/10.1016/j.ymgme.2016.12.013.

[32] A.B. Moser, N. Kreiter, L. Bezman, S. Lu, G.V. Raymond, S. Naidu, H.W. Moser, Plasma very long chain fatty acids in 3,000 peroxisome disease patients and 29,000 controls, Ann. Neurol. 45 (1999) 100–110, https://doi.org/10.1002/1531-8249(199901)45:1<100::aid-art16>3.0.co;2-u.

[33] W.C. Hubbard, A.B. Moser, A.C. Liu, R.O. Jones, S.J. Steinberg, F. Lorey, S.R. Panny, R.F. Vogt, D. Macaya, C.T. Turgeon, S. Tortorelli, G.V. Raymond, Newborn screening for X-linked adrenoleukodystrophy (X-ALD): validation of a combined liquid chromatography-tandem mass spectrometric (LC-MS/MS) method, Mol. Genet. Metab. 97 (2009) 212–220, https://doi.org/10.1016/j.ymgme.2009.03.010.

[34] K. Herzog, M.L. Pras-Raves, M.A. Vervaart, A.C. Luyf, A.C. van Kampen, R.J. Wanders, H.R. Waterham, F.M. Vaz, Lipidomic analysis of fibroblasts from Zellweger spectrum disorder patients identifies disease-specific phospholipid ratios, J. Lipid Res. 57 (2016) 1447–1454, https://doi.org/10.1194/jlr.M067470.

[35] M. Igarashi, H.H. Schaumburg, J. Powers, Y. Kishmoto, E. Kolodny, K. Suzuki, Fatty acid abnormality in adrenoleukodystrophy, J. Neurochem. 26 (1976) 851–860, https://doi.org/10.1111/j.1471-4159.1976.tb04462.x.

[36] F. Valianpour, J.J. Selhorst, L.E. van Lint, A.H. van Gennip, R.J. Wanders, S. Kemp, Analysis of very long-chain fatty acids using electrospray ionization mass spectrometry, Mol. Genet. Metab. 79 (2003) 189–196, https://doi.org/10.1016/s1096-7192(03)00098-2.

[37] M. Engelen, S. Kemp, M. de Visser, B.M. van Geel, R.J. Wanders, P. Aubourg, B.T. Poll-The, X-linked adrenoleukodystrophy (X-ALD): clinical presentation and guidelines for diagnosis, follow-up and management, Orphanet J. Rare Dis. 13 (2012) 7–51, https://doi.org/10.1186/1750-1172-7-51.

[38] I. Ferrer, J.P. Aubourg, A. Pujol, General aspects and neuropathology of X-linked adrenoleukodystrophy, Brain Pathol. 20 (2010) 817–830, https://doi.org/10.1111/j.1750-3639.2010.00390.x.

[39] A.S. Paintlia, A.G. Gilg, M. Khan, A.K. Singh, E. Barbosa, I. Singh, Correlation of very long chain fatty acid accumulation and inflammatory disease progression in childhood X-ALD: implications for potential therapies, Neurobiol. Dis. 14 (2003) 425–439, https://doi.org/10.1016/j.nbd.2003.08.013.

[40] C.R. Vargas, M. Wajner, L.R. Sirtori, L. Goulart, M. Chiochetta, D. Coelho, A. Latini, S. Llesuy, A. Bello-Klein, R. Giugliani, M. Deon, C.F. Mello, Evidence that oxidative stress is increased

in patients with X-linked adrenoleukodystrophy, Biochim. Biophys. Acta 1688 (2004) 26–32, https://doi.org/10.1016/j.bbadis.2003.10.004.

[41] S. Kemp, I.C. Huffnagel, G.E. Linthorst, R.J. Wanders, M. Engelen, Adrenoleukodystrophy - neuroendocrine pathogenesis and redefinition of natural history, Nat. Rev. Endocrinol. 12 (2016) 606–615, https://doi.org/10.1038/nrendo.2016.90.

[42] M. Baarine, P. Andréoletti, A. Athias, T. Nury, A. Zarrouk, K. Ragot, A. Vejux, J.M. Riedinger, Z. Kattan, G. Bessede, D. Trompier, S. Savary, M. Cherkaoui-Malki, G. Lizard, Evidence of oxidative stress in very long chain fatty acid-treated oligodendrocytes and potentialization of ROS production using RNA interference-directed knockdown of ABCD1 and ACOX1 peroxisomal proteins, Neuroscience 213 (2012) 1–18, https://doi.org/10.1016/j.neuroscience.2012.03.058.

[43] S. Hein, P. Schönfeld, S. Kahlert, G. Reiser, Toxic effects of X-linked adrenoleukodystrophy-associated, very long chain fatty acids on glial cells and neurons from rat hippocampus in culture, Hum. Mol. Genet. 17 (2008) 1750–1761, https://doi.org/10.1093/hmg/ddn066.

[44] M. Doria, T. Nury, D. Delmas, T. Moreau, G. Lizard, A. Vejux, Protective function of autophagy during VLCFA-induced cytotoxicity in a neurodegenerative cell model, Free Radic. Biol. Med. 137 (2019) 46–58, https://doi.org/10.1016/j.freeradbiomed.2019.04.016.

[45] T. Nury, M. Doria, G. Lizard, A. Vejux, Docosahexaenoic acid attenuates mitochondrial alterations and oxidative stress leading to cell death induced by very long-chain fatty acids in a mouse oligodendrocyte model, Int. J. Mol. Sci. 21 (2020) 641, https://doi.org/10.3390/ijms21020641.

[46] M. Baarine, K. Ragot, A. Athias, T. Nury, Z. Kattan, E.C. Genin, P. Andreoletti, F. Ménétrier, J.M. Riedinger, M. Bardou, G. Lizard, Incidence of Abcd1 level on the induction of cell death and organelle dysfunctions triggered by very long chain fatty acids and TNF-α on oligodendrocytes and astrocytes, Neurotoxicology 33 (2012) 212–228, https://doi.org/10.1016/j.neuro.2011.10.007.

[47] J. López-Erauskin, J. Galino, M. Ruiz, J.M. Cuezva, I. Fabregat, D. Cacabelos, J. Boada, J. Martínez, I. Ferrer, R. Pamplona, F. Villarroya, M. Portero-Otín, S. Fourcade, A. Pujol, Impaired mitochondrial oxidative phosphorylation in the peroxisomal disease X-linked adrenoleukodystrophy, Hum. Mol. Genet. 22 (2013) 3296–3305, https://doi.org/10.1093/hmg/ddt186.

[48] M.C. van de Beek, R. Ofman, I. Dijkstra, F. Wijburg, M. Engelen, R. Wanders, S. Kemp, Lipid-induced endoplasmic reticulum stress in X-linked adrenoleukodystrophy, Biochim. Biophys. Acta Mol. Basis Dis. 1863 (2017) 2255–2265, https://doi.org/10.1016/j.bbadis.2017.06.003.

[49] J. Zhou, M.R. Terluk, P.J. Orchard, J.C. Cloyd, R.V. Kartha, N-Acetylcysteine reverses the mitochondrial dysfunction induced by very long-chain fatty acids in Murine Oligodendrocyte model of adrenoleukodystrophy, Biomedicines 9 (2021) 1826, https://doi.org/10.3390/biomedicines9121826.

[50] J. López-Erauskin, J. Galino, P. Bianchi, S. Fourcade, A.L. Andreu, I. Ferrer, C. Muñoz-Pinedo, A. Pujol, Oxidative stress modulates mitochondrial failure and cyclophilin D function in X-linked adrenoleukodystrophy, Brain 135 (2012) 3584–3598, https://doi.org/10.1093/brain/aws292.

[51] A. Zarrouk, A. Vejux, T. Nury, H.I. El Hajj, M. Haddad, M. Cherkaoui-Malki, J.M. Riedinger, M. Hammami, G. Lizard, Induction of mitochondrial changes associated with oxidative stress on very long chain fatty acids (C22:0, C24:0, or C26:0)-treated human neuronal cells (SK-NB-E), Oxid. Med. Cell Longev. 2012 (2012) 623257, https://doi.org/10.1155/2012/623257.

[52] H. Ali, K. Morito, R.Y. Hasi, M. Aihara, J. Hayashi, R. Kawakami, K. Kanemaru, K. Tsuchiya, K. Sango, T. Tanaka, Characterization of uptake and metabolism of very long-chain fatty acids in peroxisome-deficient CHO cells, Biochim. Biophys. Acta 1867 (2022) 159088, https://doi.org/10.1016/j.bbalip.2021.159088.

[53] T. Tsukamoto, A. Bogaki, K. Okumoto, K. Tateishi, Y. Fujiki, N. Shimozawa, Y. Suzuki, N. Kondo, T. Osumi, Isolation of a new peroxisome-deficient CHO cell mutant defective in peroxisome targeting signal-1 receptor, Biochem. Biophys. Res. Commun. 230 (1997) 402–406, https://doi.org/10.1006/bbrc.1996.5971.

[54] M. Yamasaki, N. Hashiguchi, C. Fujiwara, T. Imanaka, T. Tsukamoto, T. Osumi, Formation of peroxisomes from peroxisomal ghosts in a peroxisome-deficient mammalian cell mutant upon complementation by protein microinjection, J. Biol. Chem. 274 (1999) 35293–35296, https://doi.org/10.1074/jbc.274.50.35293.

[55] E.G. Bligh, W.J. Dyer, A rapid method of total lipid extraction and purification, Can. J. Biochem. Physiol. 37 (1959) 911–917, https://doi.org/10.1139/o59-099.

[56] J. Zeng, S. Deng, Y. Wang, P. Li, L. Tang, Y. Pang, Specific inhibition of acyl-CoA oxidase-1 by an acetylenic acid improves hepatic lipid and reactive oxygen species (ROS) metabolism in

rats fed a high fat diet, J. Biol. Chem. 292 (2017) 3800–3809, https://doi.org/10.1074/jbc.M116.763532.

[57] C. Chu, L.F. Mao, H. Schulz, Estimation of peroxisomal beta-oxidation in rat heart by a direct assay of acyl-CoA oxidase, Biochem. J. 302 (1994) 23–29, https://doi.org/10.1042/bj3020023.

[58] M. Morita, S. Shinbo, A. Asahi, T. Imanaka, Very long chain fatty acid β-oxidation in astrocytes: contribution of the ABCD1-dependent and -independent pathways, Biol. Pharm. Bull. 35 (2012) 1972–1979, https://doi.org/10.1248/bpb.b12-00411.

[59] H. Singh, N. Derwas, A. Poulos, Beta-oxidation of very-long-chain fatty acids and their coenzyme A derivatives by human skin fibroblasts, Arch. Biochem. Biophys. 254 (1987) 526–533, https://doi.org/10.1016/0003-9861(87)90133-0.

[60] H. Singh, N. Derwas, A. Poulos, Very long chain fatty acid beta-oxidation by subcellular fractions of normal and Zellweger syndrome skin fibroblasts, Arch. Biochem. Biophys. 257 (1987) 302–314, https://doi.org/10.1016/0003-9861(87)90570-4.

[61] I. Singh, A.E. Moser, S. Goldfischer, H.W. Moser, Lignoceric acid is oxidized in the peroxisome: implications for the Zellweger cerebro-hepato-renal syndrome and adrenoleukodystrophy, Proc. Natl. Acad. Sci. U. S. A. 81 (1984) 4203–4207, https://doi.org/10.1073/pnas.81.13.4203.

[62] R. Sandhir, M. Khan, A. Chahal, I. Singh, Localization of nervonic acid beta-oxidation in human and rodent peroxisomes: impaired oxidation in Zellweger syndrome and X-linked adrenoleukodystrophy, J. Lipid Res. 39 (1998) 2161–2171, https://doi.org/10.1016/S0022-2275(20)32471-8.

[63] M. Baes, S. Huyghe, P. Carmeliet, P.E. Declercq, D. Collen, G.P. Mannaerts, P.P.V. Veldhoven, Inactivation of the peroxisomal multifunctional protein-2 in mice impedes the degradation of not only 2-methyl-branched fatty acids and bile acid intermediates but also of very long chain fatty acids, J. Biol. Chem. 275 (2000) 16329–16336, https://doi.org/10.1074/jbc.M001994200.

[64] J.F. Lu, A.M. Lawler, P.A. Watkins, J.M. Powers, A.B. Moser, H.W. Moser, K.D. Smith, A mouse model for X-linked adrenoleukodystrophy, Proc. Natl. Acad. Sci. U. S. A. 94 (1997) 9366–9371, https://doi.org/10.1073/pnas.94.17.9366.

[65] M. Baes, P. Gressens, S. Huyghe, N.K. De, C. Qi, Y. Jia, G.P. Mannaerts, P. Evrard, V.P. Van, P.E. Declercq, J.K. Reddy, The neuronal migration defect in mice with Zellweger syndrome (Pex5 knockout) is not caused by the inactivity of peroxisomal beta-oxidation, J. Neuropathol. Exp. Neurol. 61 (2002) 368–374, https://doi.org/10.1093/jnen/61.4.368.

[66] A. Poulos, Very long chain fatty acids in higher animals--a review, Lipids 30 (1995) 1-14, https://doi.org/10.1007/BF02537036.

[67] T. Sassa, A. Kihara, Metabolism of very long-chain Fatty acids: genes and pathophysiology, Biomol. Ther. (Seoul) 22 (2014) 83-92, https://doi.org/10.4062/biomolther.2014.017.

[68] T. Plötz, A.S. von Hanstein, B. Krümmel, A. Laporte, I. Mehmeti, S. Lenzen, Structure-toxicity relationships of saturated and unsaturated free fatty acids for elucidating the lipotoxic effects in human EndoC-βH1 beta-cells, Biochim. Biophys. Acta Mol. Basis. Dis. 1865 (2019) 165525, https://doi.org/10.1016/j.bbadis.2019.08.001.

[69] S. Grösch, S. Schiffmann, G. Geisslinger, Chain length-specific properties of ceramides, Prog. Lipid Res. 51 (2012) 50–62, https://doi.org/10.1016/j.plipres.2011.11.001.

[70] Q. Raas, M.C. van de Beek, S. Forss-Petter, I.M. Dijkstra, A. Deschiffart, B.C. Freshner, T.J. Stevenson, Y.R. Jaspers, L. Nagtzaam, R.J. Wanders, M. van Weeghel, J.Y. Engelen-Lee, M. Engelen, F. Eichler, J. Berger, J.L. Bonkowsky, S. Kemp, Metabolic rerouting via SCD1 induction impacts X-linked adrenoleukodystrophy, J. Clin. Invest. 131 (2021) e142500, https://doi.org/10.1172/JCI142500.

[71] M.R. Terluk, J. Tieu, S.A. Sahasrabudhe, A. Moser, P.A. Watkins, G.V. Raymond, R.V. Kartha, Nervonic acid attenuates accumulation of very long-chain fatty acids and is a potential therapy for adrenoleukodystrophy, Neurotherapeutics 19 (2022) 1007-1017, https://doi.org/10.1007/s13311-022-01226-7.

[72] Y. Poitelon, A.M. Kopec, S. Belin, Myelin fat facts: an overview of lipids and fatty acid metabolism, Cells 9 (2020) 812, https://doi.org/10.3390/cells9040812.

[73] R. Chrast, G. Saher, K.A. Nave, M.H. Verheijen, Lipid metabolism in myelinating glial cells: lessons from human inherited disorders and mouse models, J. Lipid Res. 52 (2011) 419–434, https://doi.org/10.1194/jlr.R009761.

[74] M. Isokawa, T. Sassa, S. Hattori, T. Miyakawa, A. Kihara, Reduced chain length in myelin sphingolipids and poorer motor coordination in mice deficient in the fatty acid elongase Elovl1, FASEB Bioadv. 1 (2019) 747-759, https://doi.org/10.1096/fba.2019-00067.